NIST Special Publication 1026r1
October 2011 Revision

CFAST – Consolidated Model of Fire Growth and Smoke Transport (Version 6) Technical Reference Guide

Richard D. Peacock
Glenn P. Forney
Paul A. Reneke

http://dx.doi.org/10.6028/NIST.SP.1026r1

National Institute of Standards and Technology
U.S. Department of Commerce

NIST Special Publication 1026r1
October 2011 Revision

CFAST – Consolidated Model of Fire Growth and Smoke Transport (Version 6) Technical Reference Guide

Richard D. Peacock
Glenn P. Forney
Paul A. Reneke
Fire Research Division
Engineering Laboratory

http://dx.doi.org/10.6028/NIST.SP.1026r1

December 2014
SVN Repository Revision: *Revision* : 283

U.S. Department of Commerce
Rebecca M. Blank, Acting Secretary

National Institute of Standards and Technology
Patrick D. Gallagher, Under Secretary for Standards and Technology and Director

Disclaimer

The U. S. Department of Commerce makes no warranty, expressed or implied, to users of CFAST and associated computer programs, and accepts no responsibility for its use. Users of CFAST assume sole responsibility under Federal law for determining the appropriateness of its use in any particular application; for any conclusions drawn from the results of its use; and for any actions taken or not taken as a result of analyses performed using these tools. CFAST is intended for use only by those competent in the field of fire safety and is intended only to supplement the informed judgment of a qualified user. The software package is a computer model which may or may not have predictive value when applied to a specific set of factual circumstances. Lack of accurate predictions by the model could lead to erroneous conclusions with regard to fire safety. All results should be evaluated by an informed user.

Intent and Use

The algorithms, procedures, and computer programs described in this report constitute a methodology for predicting some of the consequences resulting from a prescribed fire. They have been compiled from the best knowledge and understanding currently available, but have important limitations that must be understood and considered by the user. The program is intended for use by persons competent in the field of fire safety and with some familiarity with personal computers. It is intended as an aid in the fire safety decision-making process.

Preface

CFAST is a two-zone fire model used to calculate the evolving distribution of smoke, fire gases and temperature throughout compartments of a constructed facility during a fire. In CFAST, each compartment is divided into two gas layers.

The modeling equations used in CFAST take the mathematical form of an initial value problem for a system of ordinary differential equations (ODEs). These equations are derived using the conservation of mass, the conservation of energy (equivalently the first law of thermodynamics), the ideal gas law and relations for density and internal energy. These equations predict as functions of time quantities such as pressure, layer height and temperatures given the accumulation of mass and enthalpy in the two layers. The CFAST model then consists of a set of ODEs to compute the environment in each compartment and a collection of algorithms to compute the mass and enthalpy source terms required by the ODEs.

In general, this document provides the technical documentation for CFAST along with significant information on validation of the model. It follows the ASTM E1355 guide for model assessment. The guide provides several areas of evaluation:

- Model and scenarios definition: CFAST is designed primarily to predict the environment within compartmented structures which results from unwanted fires. These can range from very small containment vessels, on the order of 1 m^3 to large spaces on the order of 1000 m^3. The appropriate size fire for a given application depends on the size of the compartment being modeled. A range of such validation exercises is discussed in chapter 9.

- Theoretical basis for the model: Details of the underlying theory, governing equations, correlations, and organization used in the model are presented. The process of development of the model is discussed with reference to a range of NIST memorandums, published reports, and peer-reviewed journal articles on the model. In addition to overall limitations of zone-fire modeling, limitations of the individual sub-models are discussed.

- Mathematical and numerical robustness: CFAST has been subjected to extensive use and review both internal to NIST and by users worldwide in a broad range of applications. In addition to review within NIST independent of the model developers, the model has been published in international peer-reviewed journals worldwide, and in industry-standard handbooks referenced in specific consensus standards. Besides formal internal and peer review, CFAST is subjected to continuous scrutiny because it is available to the general public and is used internationally by those involved in fire safety design and post-fire reconstruction.

- Model sensitivity: Many of the outputs from the CFAST model are relatively insensitive to uncertainty in the inputs for a broad range of scenarios. Not surprisingly, the heat release

rate is the most important variable because it provides the driving force for firedriven flows. For CFAST, the heat release rate is prescribed by the user. Thus, careful selection of the fire size is necessary for accurate predictions. Other variables related to compartment geometry such as compartment height or vent sizes, while deemed important for the model outputs, are typically more easily defined for specific design scenarios than fire related inputs.

- Model evaluation: The CFAST model has been subjected to extensive validation studies by NIST and others. Although some differences between the model and the experiments were evident in these studies, they are typically explained by limitations of the model and uncertainty of the experiments. Most prominent in the studies reviewed was the overprediction of gas temperature often attributed to uncertainty in soot production and radiative fraction. Still, studies typically show predictions accurate within about 30 % of measurements for a range of scenarios. Like all predictive models, the best predictions come with a clear understanding of the limitations of the model and of the inputs provided to the calculations.

Nomenclature

A	area, m^2
A_{slab}	cross-sectional area of vent slab in horizontal vent flow, m^2
A_v	cross-sectional area of a vent, m^2
C	vent constriction (or flow) coefficient, dimensionless
C_{LOL}	lower oxygen limit coefficient, fraction of the available fuel which can be burned with the available oxygen, dimensionless
C_T	constant from plume centerline temperature calculation, 9.115
c_p	heat capacity of air at constant pressure, J/kg K
c_v	heat capacity of air at constant volume, J/kg K
D	fire diameter, m
D^*	characteristic fire diameter parameter, $\left(Q_f/\left(\rho_\infty c_p T_\infty \sqrt{g}\right)\right)^{2/5}$
	vent diameter, m
d_0	inlet ceiling jet depth in corridor flow, m
E_O	energy release per unit mass of oxygen consumed, J/kg
E_i	internal energy in layer i, W
F_{k-j}	configuration factor, fraction of radiation given off by surface k intercepted by surface j, dimensionless
g	gravitational constant, 9.8 m/s^2
h	convective heat transfer coefficient (W/m^2 K)
$\dot{h}_i$	rate of addition of enthalpy into layer i, J/s
$\dot{h}_L$	rate of addition of enthalpy into lower layer in a compartment, J/s
$\dot{h}_U$	rate of addition of enthalpy into upper layer in a compartment, J/s
H	height of a compartment, m
	flame height, m
H_1	distance from fire source to target location in plume centerline temperature calculation, m
H_2	distance from virtual fire source to target location in plume centerline temperature calculation, m
H_c	heat of combustion of the fuel, J/kg
k	equivalent thermal conductivity of air, W/m K, with subscripts c,e and s
k	equilibrium coefficient for HCl transport and deposition
L	length of a compartment, m
	characteristic length for radiation calculation, m
M_F	molar mass of fuel, kg/mol

$M_{O_2,CO_2,...HCN,S}$	molar mass of oxygen, carbon dioxide, water, carbon monoxide, hydrochloric acid, hydrogen cyanide, and soot, kg/mol
m	mass, kg
$\dot{m}_e$	entrainment rate, kg/s
$\dot{m}_{ex}$	bi-directional vent flow in vertical flow vent, kg/s
$\dot{m}_f$	pyrolysis rate of the fire, kg/s
m_i	total mass in gas layer i, kg
$\dot{m}_{io}$	mass flow rate through a vent, kg/s
m_L	total mass in lower gas layer in a compartment, kg
$\dot{m}_O$	oxygen required for full combustion of available fuel, kg/s
$\dot{m}_p$	plume flow rate, kg/s
m_U	total mass in upper gas layer in a compartment, kg
P	pressure at floor level of a compartment, Pa
P_b	cross-vent differential pressure at the bottom of a vent flow slab in horizontal vent flow, Pa
P_t	cross-vent differential pressure at the top of a vent flow slab in horizontal vent flow, Pa
Q_{ceil}	average convective heat transfer from the ceiling jet to the ceiling surface, W
Q_f	total heat release rate of the fire, W
$Q_{f,C}$	heat release rate of the fire released as convective energy, W
$Q_{f,eq}$	effective heat release rate of a vent fire, kW
$Q_{f,R}$	heat release rate of the fire released as radiation, W
Q_{spray}	spread density of a sprinkler
$Q^*_{I,1}$	original fire strength for plume temperature calculation, dimensionless
$Q^*_{I,2}$	modified fire strength for plume temperature calculation when target location is in the upper layer, dimensionless
$\Delta\hat{q}''_k$	net radiative flux at wall segment k
q''	heat flux, W/m^2
R	universal gas conference, J/kg K
RTI	thermal characteristic response time index of a sprinkler or heat detector (m$^{1/2}$ s$^{1/2}$)
r	radial distance from the fire, m
S	vent coefficient for vertical flow vents, dimensionless
T_∞	ambient gas temperature in compartment well removed from a target, K
T_{amb}	ambient temperature, K
T_i	gas temperature of layer i, K
T_L	gas temperature of lower layer in a compartment, K
T_p	gas temperature in the plume, K
T_U	gas temperature of upper layer in a compartment, K
T_0	inlet gas temperature of the ceiling jet in corridor flow, K
T^*_1	calculated plume temperature at the transition between continuous flaming and intermittent flaming, K
T^*_2	calculated plume temperature at the transition intermittent flaming and the fire plume, K
t	time, s

V	total volume of a compartment, m^3
V_L	total volume of lower layer in a compartment, m^3
V_U	total volume of upper layer in a compartment, m^3
V_i	volume of gas layer i, m^3
v	velocity, m/s
v_0	inlet ceiling jet velocity in corridor flow, m/s
W	width of a compartment, m; wall thickness, m
Y_{LOL}	mass fraction of oxygen below which combustion will no longer occur, dimensionless
Y_{O_2}	mass fraction of oxygen in a gas layer, dimensionless
y_s	soot yield, mass of soot produced by the fire per unit mass of fuel, kg/kg
$Z_{I,1}$	distance from fire source to the interface between upper and lower layers, m
$Z_{I,2}$	distance from virtual fire source to the interface between upper and lower layers, m
z	height above the base of the fire, m
z_ν	height of the virtual origin of a vent fire, m
z_p	reduced height of the plume of a vent fire, m
z_0	height of the virtual origin of fire, m
z_1^*	height above the base of the fire at the transition between continuous flaming and intermittent flaming, m
z_2^*	height above the base of the fire at the transition intermittent flaming and the fire plume, m
α	gas absorptance, dimensionless thermal diffusivity in conduction (m^2/s)
β	experimentally-determined constant in plume centerline temperature calculation, $\beta^2 = 0.913$
γ	ratio of c_p/c_v, dimensionless
ΔT	temperature rise, K
ε	emissivity
ν	stoichiometric coefficients for combustion reaction, dimensionless kinematic viscosity, m^2/s
ρ	density, kg/m^3
ρ_∞	density of gas well removed from a target, kg/m^3
ρ_{cj}	density of the ceiling jet gas, kg/m^3
ρ_i	density of gas layer i, kg/m^3
σ	Stefan-Boltzman constant (5.67×10^{-8} W/m^2K^4)
τ	transmittance, dimensionless
χ_C	fraction of the fire's heat release rate released as convective energy, dimensionless
χ_R	fraction of the fire's heat release rate released as radiation, dimensionless
ξ	ratio of upper layer gas temperature to lower layer gas temperature, dimensionless

Acknowledgments

Continuing support for CFAST is via internal funding at NIST. In addition, support is provided by other agencies of the U.S. Federal Government, most notably the Nuclear Regulatory Commission Office of Research and the U.S. Department of Energy. The U.S. NRC Office of Research has funded key validation experiments, the preparation of the CFAST manuals, and the continuing development of sub-models that are of importance in the area of nuclear power plant safety. Special thanks to Mark Salley, David Stroup, and Jason Dreisbach for their efforts and support. Support to refine the software development and quality assurance process for CFAST has been provided by the U.S. Department of Energy (DOE). The assistance of Subir Sen and Debra Sparkman in understanding DOE software quality assurance programs and the application of the process to CFAST is gratefully acknowledged.

Doug Carpenter, Combustion Sciences and Engineering, has contributed numerous corrections, clarifications, and updates to the guides and the model through his detailed review of the model and documentation. Allan Coutts, Washington Safety Management Solutions, provided insight into the application of fire models to nuclear safety applications and detailed review of the CFAST document updates for DOE.

Contents

List of Figures

List of Tables

Chapter 1

Overview

This chapter provides a general description of the Consolidated Fire and Smoke Transport (CFAST) model following the guidance in ASTM E1355 [1].

1.1 Model Documentation

1.1.1 Name and Version of the Model

The name of the model is the Consolidated Fire Growth and Smoke Transport Model or CFAST. The first public release was version 1.0 in June, 1990. This version was restructured from FAST [2] to incorporate the "lessons learned" from the zone model CCFM developed by Cooper and Forney [3]. Version 2 was released as a component of Hazard 1.2 in 1994 [4, 5]. The first of the 3.x series was released in 1995 and included a vertical flame spread algorithm, ceiling jets and non-uniform heat loss to the ceiling, spot targets, and heating and burning of multiple objects (ignition by flux, temperature or time) in addition to multiple prescribed fires. As it evolved over the next five years, version 3 included smoke and heat detectors, suppression through heat release reduction, better characterization of flow through doors and windows, vertical heat conduction through ceiling/floor boundaries, and non-rectangular compartments. In 2000, version 4 was released and included horizontal heat conduction through walls, and horizontal smoke flow in corridors. Version 5 improved the combustion chemistry. Version 6, released in July, 2005, incorporates a more consistent implementation of vents, fire objects and event processing and includes a graphical user interface which substantially improves its usability.

1.1.2 Type of Model

CFAST is a two-zone fire model that predicts the thermal environment within compartmented structures resulting from a fire. Each compartment is divided into an upper and lower gas layer. The fire drives combustion products from the lower to the upper layer via the plume. The temperature within each layer is uniform, and its evolution in time is described by a set of ordinary differential equations.

1.1.3 Model Developers

CFAST was developed and is maintained primarily by the Fire Research Division of the National Institute of Standards and Technology. The developers are Walter Jones, Richard Peacock, Glenn Forney, Rebecca Portier, Paul Reneke, and John Hoover [1].

There have been contributions through research and published papers at Worcester Polytechnic Institute, University of California at Berkeley, VTT of Finland and CITCM of France. An important guide to development of the model has been from many people around the world who have provided ideas, suggestions, comments, detailed questions, opinions on what should happen in particular scenarios, what physics and chemistry are needed and what types of problems must be addressed by such a model in order to be useful for real world applications.

1.1.4 Relevant Publications

To accompany the model and simplify its use, NIST has developed this Technical Reference Guide [6], a User's Guide [7] and a Software and Validation Guide [8]. The Technical Reference Guide describes the underlying physical principles and summarizes sensitivity analysis, model validation, and model limitations consistent with ASTM E 1355 [1]. The Users Guide describes how to use the model.

The U.S. Nuclear Regulatory Commission has published a verification and validation study of five selected fire models commonly used in support of risk-informed and performance-based fire protection at nuclear power plants [9]. In addition to an extensive study of the CFAST model, the report compares the output of several other models ranging from simple hand calculations to more complex CFD codes such as the Fire Dynamics Simulator (FDS) developed by NIST.

There are documents available (http://cfast.nist.gov) that are applicable to versions 2, 3, 5 as well as 6 of both the model and user interface.

1.1.5 Governing Equations and Assumptions

For CFAST, as for most zone fire models, the equations solved are for conservation of mass and energy. The momentum equation is not solved explicitly, except for use of the Bernoulli equation for the flow velocity at vents. Based on an integration over the volume of an element, these equations are solved as ordinary differential equations.

There are two assumptions which reduce the computation time dramatically. The first is that relatively few zones or elements per compartment is sufficient to model the physical situation. The second assumption is to close the set of equations without using the momentum equation in the compartment interiors. This simplification eliminates acoustic waves. Though this prevents one from calculating gravity waves in compartments (or between compartments), coupled with only a few elements per compartment allows for a prediction in a large and complex space very quickly.

1.1.6 Input Data Required to Run the Model

All of the data required to run the CFAST model reside in a primary data file, which the user creates. Some instances may require databases of information on objects, thermophysical proper-

[1] Naval Research Laboratory, Washington, DC 20375.

ties of boundaries, and sample prescribed fire descriptions. In general, the data files contain the following information:

- compartment dimensions (height, width, length)
- construction materials of the compartment (e.g., concrete, gypsum)
- material properties (e.g., thermal conductivity, specific heat, density, thickness, heat of combustion)
- dimensions and positions of horizontal and vertical flow openings such as doors, windows, and vents
- mechanical ventilation specifications
- fire properties (e.g., heat release rate, lower oxygen limit, and species production rates as a function of time)
- sprinkler and detector specifications
- positions, sizes, and characteristics of targets

The input files are provided for the validation exercises described in the Validation Guide [8]. These examples range from simple one-compartment simulations to a large multi-story hotel scenario that includes an elevator shaft and stairwell pressurization. A complete description of the input parameters required by CFAST can be found in the CFAST User's Guide [7]. Some of these parameters have default values included in the model, which are intended to be representative for a range of fire scenarios.

1.1.7 Property Data

Any simulation of a real fire scenario involves prescribing material properties for the walls, floor, ceiling, and furnishings. CFAST treats all of these materials as homogeneous solids, thus the physical parameters for many real objects can only be viewed as approximations to the actual properties. Describing these materials in the input data file is a challenging task for the model user. Thermal properties for the most common barrier materials used in construction, e.g. gypsum wall board, are included in a database, thermal.df, included with the model. These properties come directly from handbook values for typical materials [10].

1.1.8 Model Results

The output of CFAST are the sensible variables that are needed for assessing the environment in a building subjected to a fire. Once the simulation is complete, CFAST produces an output file containing all of the solution variables. Typical outputs include (but are not limited to) the following:

- environmental conditions in the room (such as hot gas layer temperature; plume centerline temperature; oxygen and smoke concentration; and ceiling, wall, and floor temperatures)

- heat transfer-related outputs to walls and targets (such as incident convective, radiated, and total heat fluxes)
- fire intensity and flame height
- flow velocities through vents and openings
- detector and sprinkler activation times

There is more extensive discussion of the output in chapter 6 of this technical reference manual and the user's guide. The output is always in the metric system of units.

1.1.9 Uses and Limitations of the Model

CFAST has been developed for use in solving practical fire problems in fire protection engineering. It is intended for use in system modeling of building and building components. A priori prediction of flame spread or fire growth on objects is not modeled. Rather, the consequences of a specified fire is estimated. It is not intended for detailed study of flow within a compartment, such as is needed for smoke detector siting. It includes the activation of sprinklers and fire suppression by water droplets.

The most extensive use of the model is in fire and smoke spread in complex buildings. The efficiency and computational speed are inherent in the few computation cells needed for a zone model implementation. The use is for design and reconstruction of time-lines for fire and smoke spread in residential, commercial, and industrial fire applications. Some applications of the model have been for design of smoke control systems.

- Compartments: CFAST is generally limited to situations where the compartment volumes are strongly stratified. However, in order to facilitate the use of the model for preliminary estimates when a more sophisticated calculation is ultimately needed, there are algorithms for corridor flow, smoke detector activation, and detailed heat conduction through solid boundaries. This model does provide for non-rectangular compartments, although the application is intended to be limited to relatively simple spaces. There is no intent to include complex geometries where a complex flow field is a driving force. For these applications, computational fluid dynamics (CFD) models are appropriate.
- Gas Layers: There are also limitations inherent in the assumption of stratification of the gas layers. The zone model concept, by definition, implies a sharp boundary between the upper and lower layers, whereas in reality, the transition is typically over about 10 % of the height of the compartment and can be larger in weakly stratified flow. For example, a burning cigarette in a normal room is not within the purview of a zone model. While it is possible to make predictions within 5 % of the actual temperatures of the gas layers, this is not the optimum use of the model. It is more properly used to make estimates of fire spread (not flame spread), smoke detection and contamination, and life safety calculations.
- Heat Release Rate: CFAST does not predict fire growth on burning objects. Heat release rate is specified by the user for one or more fire objects. The model does include the ability to limit the specified burning based on available oxygen. There are also limitations inherent

in the assumptions used in application of the empirical models. As a general guideline, the heat release should not exceed about 1 MW/m^3. This is a limitation on the numerical routines attributable to the coupling between gas flow and heat transfer through boundaries (conduction, convection, and radiation). The inherent two-layer assumption is likely to break down well before this limit is reached.

- Radiation: Because the model includes a sophisticated radiation model and ventilation algorithms, it has further use for studying building contamination through the ventilation system, as well as the stack effect and the effect of wind on air circulation in buildings. Radiation from fires is modeled with a simple point source approximation. This limits the accuracy of the model near fire sources. Calculation of radiative exchange between compartments is not modeled.

- Ventilation and Leakage: In a single compartment, the ratio of the volume of the compartment to the area of vents connecting the compartment to another should not exceed roughly 2 m. This is a limitation on the plug flow assumption for vents. A more important limitation arises from the uncertainty in the scenario specification. For example, leakage in buildings is significant, and this affects flow calculations especially when wind is present and for tall buildings. These effects can overwhelm limitations on accuracy of the implementation of the vent flow model. The overall accuracy of the model is closely tied to the specificity, care, and completeness with which the data are provided.

- Thermal Properties: The accuracy of the model predictions is limited by how well the user can specify the thermophysical properties. For example, the fraction of fuel which ends up as soot has an important effect on the radiation absorption of the gas layer and, therefore, the relative convective versus radiative heating of the layers and walls, which in turn affects the buoyancy and flow. There is a higher level of uncertainty of the predictions if the properties of real materials and real fuels are unknown or difficult to obtain, or the physical processes of combustion, radiation, and heat transfer are more complicated than their mathematical representations in CFAST.

User feedback indicates that using CFAST to predict the transport of heat and combustion products from a prescribed fire is straightforward, easily and quickly accomplished, and the results are within expectations. Any user of a computer based (numerical) model must be aware of the assumptions and approximations being employed. Except for those few materials supplied in the property databases, the user must supply the thermal properties of the materials, and then assess the performance of the model compared with experiments to ensure that the model is valid for a specific application. Only then can the model be expected to predict the outcome of fire scenarios that are similar to those that have actually been tested.

In addition, there are specific limitations and assumptions made in the development of the algorithms. These are detailed in the discussion of each of these sub-models:

In addition, there are specific limitations and assumptions made in the development of the algorithms. These are detailed in the discussion of each of these sub-models:

- section **??** on zone model assumptions,

- section 3 on prescribed fires,

- section 3.5 on the relationship between fires and mass balance,
- section **??** on the plume entrainment model,
- section **??** on the assumptions made for corridor flow correlations,
- section 5.0.4 on the assumptions made for radiation heat transfer,
- section 6.2 on the suppression model, and
- section 6.3.2 on HCl deposition.

1.2 Scenarios for which the Model is Evaluated in this Document

CFAST is used for a wide range of buildings of interest, from glove-box size compartments, to complex hotels to the vehicle assembly building at Cape Canaveral. The intended use of ASTM E1355 [1] is to validate a specific scenario of interest so that the model can be used for scenarios similar to the chosen scenario. The intent of this document, however, is to cover a much wider range of scenarios which encompass the range of acceptable use of the model. Thus, this section provides a description of this broader range of scenarios as discussed in this technical reference guide rather than a single, specific scenario of interest for a validation exercise.

1.2.1 Description of Scenarios of Interest

CFAST is designed primarily to predict the environment within compartmented structures which results from unwanted fires. These can range from very small containment vessels, on the order of 1 m^3 to large spaces on the order of 1000 m^3. As discussed in the section on limitations and use (see section 1.1.9), the appropriate size fire depends on the size of the compartment being modeled. A range of such validation exercises is discussed in chapter 9.

1.2.2 List of Quantities Predicted by the Model

CFAST provides a prediction of the plume centerline, gas layer, and boundary temperatures, target temperatures, species concentration (including soot volume fraction), layer height, fire size and flame length, floor pressure, flow and fire size at vents, and heat flux (both radiative and convective). There is a more extensive discussion of the output in the CFAST user's guide.

1.2.3 Degree of Accuracy Required for Each Output Quantity

The degree of accuracy for each output variable required by the user is highly dependent on the technical issues associated with the analysis. The user must ask: How accurate does the analysis have to be to answer the technical question posed? Thus, a generalized definition of the accuracy required for each quantity with no regard as to the specifics of a particular analysis is not practical and would be limited in its usefulness.

Returning to the earlier definitions of "design" and "reconstruction," fire scenarios, design applications typically are more accurate because the heat release rate is prescribed rather than predicted, and the initial and boundary conditions are far better characterized. Mathematically, a design calculation is an example of a "well-posed" problem in which the solution of the governing equations is advanced in time starting from a known set of initial conditions and constrained by a known set of boundary conditions. The accuracy of the results is a function of the fidelity of the numerical solution, which is largely dependent on the quality of the model inputs.

A reconstruction is an example of an "ill-posed" problem because the outcome is known whereas the initial and boundary conditions are not. There is no single, unique solution to the problem. Rather, it is possible to simulate numerous fires that produce the given outcome. There is no right or wrong answer, but rather a small set of plausible fire scenarios that are consistent with the collected evidence and physical laws incorporated into the model. These simulations are then used to demonstrate why the fire behaved as it did based on the current understanding of fire physics incorporated in the model. Most often, the result of the analysis is only qualitative. If there is any quantification at all, it could be in the time to reach critical events, like a roof collapse or room flashover.

The CFAST validation guide [8] includes efforts to date involving well-characterized geometries and prescribed fires. These studies show that CFAST predictions vary from being within experimental uncertainty to being about 30 % different than measurements of temperature, heat flux, gas concentration, *etc* (see, for example, reference [9]). In general, this is adequate for its intended uses which are life-safety calculations and estimation of the environment to which building elements are subjected in a fire environment. Applied design margins are typically larger than this level of accuracy and may be appropriate to insure an adequate factor of safety.

1.3 Review of the Theoretical Development of the Model

Details of the software quality assurance process for CFAST is included in the Software and Model Evaluation Guide [8]. This section provides a summary of this process The current version of ASTM E 1355-04 includes provisions to guide in the assessment of the theoretical basis of the model that includes a review of the model "by one or more recognized experts fully conversant with the chemistry and physics of fire phenomenon, but not involved with the production of the model. Publication of the theoretical basis of the model in a peer-reviewed journal article may be sufficient to fulfill this review? [1].

CFAST has been subjected to independent review in two ways, internal and external. First, all documents issued by the National Institute of Standards and Technology receive three levels of internal review by members of the staff not involved in the preparation of the report or underlying research. The theoretical basis of CFAST is presented in this document, and is subject to internal review by staff members who are not active participants in the development of the model, but who are members of the Fire Research Division and are considered experts in the fields of fire and combustion. The same was true of previous versions of the technical reference guide over the last decade [2, 11, 12]. Externally, the theoretical basis for the model has been published in peer reviewed journals [13, 14, 15] and conference proceedings [16]. In addition, CFAST is used worldwide by fire protection engineering firms who review the technical details of the model related to their particular application. Some of these firms also publish in the open literature reports

documenting internal efforts to validate the model for a particular use. Many of these studies are discussed in more detail in the present document.

In addition to the formal review, procedures were in place during the development of CFAST to assure the quality of the model. These procedures included several components:

- Review of proposed changes to the code by at least two others involved in the development process to insure that a proposed change was consistent with the rest of the CFAST code and was implemented correctly. These reviews, while informal in nature, provided a comprehensive review of the changes to the model during its development. Significant changes were documented in internal memorandums covering such areas as the numerics and structure of the model [17], improvements in the chemistry [18], convection [19], HCl deposition [20] algorithms, and output formats for the model [21]. Comparisons of the impact of the changes on the output results were often described in internal memorandums (see, for example, reference [17]).

- Internal review of the model prior to public release. In addition to the normal NIST document review process, the CFAST software was circulated internally to Fire Research Division Staff to allow interested staff members to test the model [22, 23, 24]. These memorandums detail changes to the model since the last public release of the model and provide documentation of the history of the model development.

- For each major release of CFAST, NIST has maintained a history of the source code which goes back to March 1989. While it is not practical to reconstruct the programs for each release for use with modern software tools and computer operating systems, the source code history allows the developers to examine what changes were made at each release point. This provides detailed documentation of the history of model development and is often useful to understand the impact of changes to submodels over the development of the model.

- Once a release of CFAST was approved by NIST, it was announced with a letter to model users which provided a summary of model changes and available documentation. In essence, these were a condensation of the internal memorandums, without details or printout of specific code changes. These memorandums provide documentation of the history of the model development [25, 26, 27, 28, 29].

Finally, CFAST has been reviewed and included in industry-standard handbooks such as the SFPE Handbook [30] and referenced in specific standards, including NFPA 805 [31] and NFPA 551 [32].

1.3.1 Assessment of the Completeness of Documentation

There are three primary documents on CFAST, this Technical Reference Guide, the User?s Guide [7], and the Software Development and Model Evaluation Guide [8]. This document is the Technical Reference Guide and provides documentation of the governing equations, assumptions, and approximations of the various submodels. It also includes a summary description of the model structure, and numerics. The Model User?s Guide includes a description of the model input data

requirements and model results. The Software Development and Model Evaluation Guide describes the software quality assurance process used in the development and maintenance of the model and includes an extensive discussion of the validation of the model.

The extensive formal review process for all NIST publications in part insures the quality of the CFAST Guides. In addition, the model developers routinely receive feedback from users on the completeness of the documentation and add clarifications when needed. It is estimated that there are several thousand users of CFAST. Before new versions of the model are released, there is a "beta test" period in which the users test the new version using the updated documentation. This process is similar, although less formal, to that which most computer software programs undergo. Training courses for use of the model in fire hazard analysis have been developed from the model documentation and presented at training courses worldwide [33].

1.3.2 Assessment of Justification of Approaches and Assumptions

The technical approach and assumptions of the model have been presented in the peer reviewed scientific literature and at technical conferences. Also, all documents released by NIST are required to go through an internal editorial review and approval process. This process is designed to ensure compliance with the technical requirements, policy, and editorial quality required by NIST. The technical review includes a critical evaluation of the technical content and methodology, statistical treatment of data, uncertainty analysis, use of appropriate reference data and units, and bibliographic references. CFAST manuals are always first reviewed by a member of the Fire Research Division, then by the immediate supervisor of the author of the document, then by the chief of the Fire Research Division, and finally by a reader from outside the division. Both the immediate supervisor and the division chief are technical experts in the field. Once the document has been reviewed, it is then brought before the Editorial Review Board (ERB), a body of representatives from all the NIST laboratories. At least one reader is designated by the Board for each document that it accepts for review. This last reader is selected based on technical competence and impartiality. The reader is usually from outside the division producing the document and is responsible for checking that the document conforms with NIST policy on units, uncertainty and scope. This reader does not need to be a technical expert in fire or combustion.

Besides formal internal and peer review, CFAST is subjected to continuous scrutiny because it is available to the general public and is used internationally by those involved in fire safety design and postfire reconstruction. The source code for CFAST is also released publicly, and has been used at various universities worldwide, both in the classroom as a teaching tool as well as for research. As a result, flaws in the theoretical development and the computer program itself have been identified and fixed. The user base continues to serve as a means to evaluate the model, which is as important to its development as the formal internal and external peer review processes.

1.3.3 Assessment of Constants and Default Values

A comprehensive assessment of the numerical parameters (such as default time step or solution convergence criteria) and physical parameters (such as empirical constants for convective heat transfer or plume entrainment) used in CFAST is not available in one document. Instead, specific parameters have been tested in various verification and validation studies performed at NIST and elsewhere. Numerical parameters are described in this Technical Reference Guide and are subject

to the internal review process at NIST, but many physical parameters are extracted from the literature and do not undergo a formal review. In addition, default values for the various model inputs have been specifically reviewed by a professional fire protection engineering university professor to insure appropriate default values and suggested limits for the various input values. The model user is expected to assess the appropriateness of default values provided by CFAST and make changes to the default values if need be.

Chapter 2

The Basic Transport Equations

The equations used in CFAST take the form of an initial value problem for a system of ordinary differential equations. These equations are derived from the conservation laws of mass and energy (equivalently the first law of thermodynamics) and the ideal gas law. These equations predict as functions of time quantities such as pressure, layer height and temperatures given the gains and losses of mass and energy in the two layers. The assumption of a zone model is that properties such as temperature can be approximated throughout a control volume by an average value. Many formulations based upon these assumptions can be derived. Though equivalent mathematically, these formulations differ in their numerical solution.

The exchange of mass and enthalpy between zones is due to physical phenomena such as fire plumes, natural and forced ventilation, convective and radiative heat transfer, and so on. For example, a vent exchanges mass and enthalpy between zones in connected rooms, a fire plume typically adds heat to the upper layer and transfers entrained mass and enthalpy from the lower to the upper layer, and convection transfers enthalpy from the gas layers to the surrounding walls.

It is assumed that each compartment is divided into two control volumes, a relatively hot upper layer and a relatively cool lower layer, as illustrated in Fig. 2.1. The gas temperature and density are assumed constant in each layer. The compartment as a whole is assumed to have a single value of pressure, P. It is also assumed that all thermodynamic parameters are constant. The specific heat at constant volume and at constant pressure, c_v and c_p, the universal gas constant, R, and the ratio of specific heats, γ, are related by $\gamma = c_p/c_v$ and $R = c_p - c_v$. For ambient air, $c_p \approx 1$ kJ/(kg $\cdot$ K) and $\gamma = 1.4$. Conservation of mass in each layer, $\dot{m}_i$, is expressed

$$\frac{dm_i}{dt} = \dot{m}_i \tag{2.1}$$

Conservation of energy takes the form of the first law of thermodynamics, which states that the rate of increase of internal energy plus the rate at which the layer does work by expansion is equal to the rate at which enthalpy is added to the gas:

$$\frac{d(c_v m_i T_i)}{dt} + P\frac{dV_i}{dt} = \dot{h}_i \tag{2.2}$$

The enthalpy source term, $\dot{h}_i$, consists of the fire's heat release rate, conduction losses to walls, and radiation exchange. The layer temperature and mass are related to the layer volume and compartment pressure via the ideal gas law:

$$PV_i = m_i R T_i \tag{2.3}$$

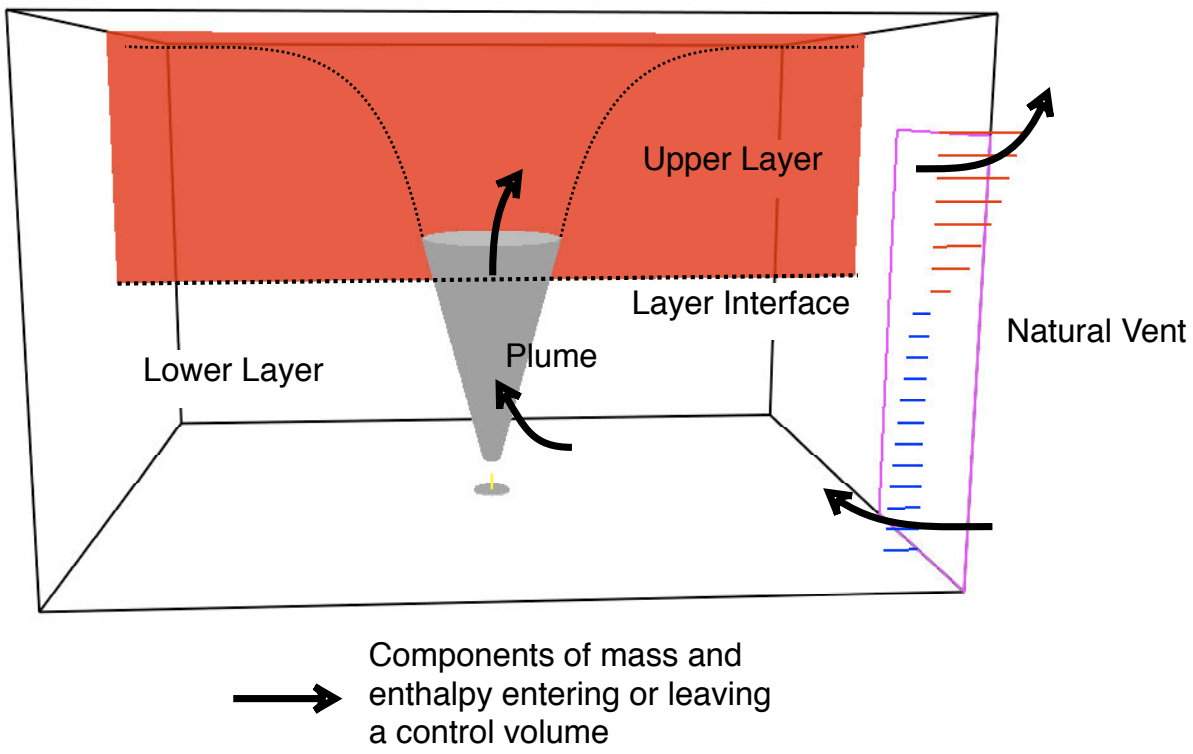

Figure 2.1: Schematic of control volumes in a two-layer zone model.

A system of ordinary differential equations for the compartment pressure, upper layer volume, and layer temperatures can be derived from these three basic principles:

$$\frac{dP}{dt} = \frac{\gamma-1}{V}\left(\dot{h}_\mathrm{l}+\dot{h}_\mathrm{u}\right) \tag{2.4}$$

$$\frac{dV_\mathrm{u}}{dt} = \frac{1}{P\gamma}\left((\gamma-1)\,\dot{h}_\mathrm{u}-V_\mathrm{u}\frac{dP}{dt}\right) \tag{2.5}$$

$$\frac{dT_\mathrm{u}}{dt} = \frac{1}{c_p m_\mathrm{u}}\left(\dot{h}_\mathrm{u}-c_p\dot{m}_\mathrm{u}T_\mathrm{u}+V_\mathrm{u}\frac{dP}{dt}\right) \tag{2.6}$$

$$\frac{dT_\mathrm{l}}{dt} = \frac{1}{c_p m_\mathrm{l}}\left(\dot{h}_\mathrm{l}-c_p\dot{m}_\mathrm{u}T_\mathrm{l}+V_\mathrm{l}\frac{dP}{dt}\right) \tag{2.7}$$

As discussed in Refs. [34] and [35], these equations are stiff, meaning that the pressure adjusts to changing conditions more quickly than the other variables. Runge-Kutta methods or predictor-corrector methods such as Adams-Bashforth require prohibitively small time steps in order to track the short time scale phenomena (pressure in our case). Methods that calculate the Jacobian (or at least approximate it) have a much larger stability region for stiff problems and are thus more successful at their solution.

Chapter 3

The Fire Plume

Fires in CFAST are specified by the user in terms of a time-dependent heat release rate (HRR), an effective fuel molecule, and the yields of the products of incomplete combustion like soot and CO. Fires can be specified in multiple compartments and are treated as totally separate entities, with no interaction of the plumes. These fires are generally referred to as "objects" and can be ignited at a prescribed time, temperature or heat flux.

CFAST does not include a pyrolysis model to *predict*, as opposed to specify, the growth and spread of the fire. Rather, pyrolysis rates for each fire are prescribed by the user. While this approach does not directly account for increased pyrolysis due to radiative feedback from the flame or compartment, in theory these effects could be prescribed by the user. In an actual fire, this is an important consideration, and the specification used should consider the experimental conditions as closely as possible.

3.1 Combustion Chemistry

The HRR of the fire is specified by the user, but it may be constrained by the availability of oxygen in the compartment. The combustion of a hydrocarbon fuel is described by the following single-step reaction:

$$\begin{aligned} \mathrm{C_{n_C}H_{n_H}O_{n_O}N_{n_N}Cl_{n_{Cl}}} \;+\; \nu_{\mathrm{O_2}}\,\mathrm{O_2} \rightarrow \\ \nu_{\mathrm{CO_2}}\,\mathrm{CO_2} \;+\; \nu_{\mathrm{H_2O}}\,\mathrm{H_2O} + \nu_{\mathrm{CO}}\,\mathrm{CO} + \nu_{\mathrm{S}}\,\mathrm{Soot} + \nu_{\mathrm{HCl}}\mathrm{HCl} + \nu_{\mathrm{HCN}}\mathrm{HCN} \end{aligned} \tag{3.1}$$

The user specifies the composition of the fuel molecule and the yields of soot and CO, y_{S} and y_{CO}, which are related to their stoichiometric coefficients as follows:

$$\nu_{\mathrm{S}} = \frac{M_{\mathrm{F}}}{M_{\mathrm{S}}}\, y_{\mathrm{S}} \tag{3.2}$$

$$\nu_{\mathrm{CO}} = \frac{M_{\mathrm{F}}}{M_{\mathrm{CO}}}\, y_{\mathrm{CO}} \tag{3.3}$$

Under the assumption that all of the nitrogen and chlorine in the fuel are converted to HCN and HCl, the other stoichiometric coefficients are:

$$\nu_{\mathrm{CO_2}} = \mathrm{n_C} - (\nu_{\mathrm{CO}} + \nu_{\mathrm{HCN}} + \nu_{\mathrm{S}}) \tag{3.4}$$

$$\nu_{H_2O} = \frac{n_H - (\nu_{HCl} + \nu_{HCN})}{2} \tag{3.5}$$

$$\nu_{O_2} = \nu_{CO_2} + \frac{\nu_{H_2O} + \nu_{CO} - n_O}{2} \tag{3.6}$$

$$\nu_{HCl} = n_{Cl} \tag{3.7}$$

$$\nu_{HCN} = n_N \tag{3.8}$$

Note that the nitrogen in the air acts only as a diluent. The yields of hydrogen cyanide and hydrogen chloride are based solely on the composition of the fuel molecule. Finally, a user-specified trace species can be specified to follow the transport that results from fire-induced flow for an arbitrary species. This may be of particular interest for radiological releases [36], but may be useful for any trace amounts released by a fire.

3.2 Heat Release Rate

As fuel and oxygen are consumed, heat is released and various products of combustion are formed. The heat is released as radiation and convected enthalpy:

$$\dot{Q}_r = \chi_r \dot{Q} \tag{3.9}$$

$$\dot{Q}_c = (1 - \chi_r) \dot{Q} \tag{3.10}$$

where, χ_r is the fraction of the fire's heat release rate given off as radiation. The default value to 0.30 [37].

While it is convenient for the user to directly specify the heat release rate of the fire, it is actually the pyrolysis rate of fuel, $\dot{m}_f$, that is specified:

$$\dot{m}_f = \frac{\dot{Q}}{\Delta h} \tag{3.11}$$

where Δh is the heat of combustion. In the event that the HRR is constrained by the availability of oxygen, the pyrolysis rate does not change, but the HRR becomes:

$$\dot{Q} = \min\left(\dot{m}_f \Delta h \, , \, \dot{m}_e Y_{O_2} C_{LOL} \Delta h_{O_2}\right) \tag{3.12}$$

where $\dot{m}_e$ is the entrainment rate, Y_{O_2} is the mass fraction of oxygen in the layer containing the fire, Δh_{O_2} is the heat of combustion based on oxygen consumption[1], and C_{LOL} is the smoothing function ranging from 0 to 1:

$$C_{LOL} = \frac{\tanh\left(800(Y_{O_2} - Y_{O_2,l}) - 4\right) + 1}{2} \tag{3.13}$$

The limiting oxygen mass fraction, $Y_{O_2,l}$, is 0.1, by default.

[1] The heat of combustion based on oxygen consumption is taken to be 13.1 MJ/kg, representative of typical hydrocarbon fuels [38].

3.3 Plume Entrainment

The mass entrainment of air into the plume, $\dot{m}_\mathrm{e}$, is estimated using either McCaffrey's [39] or Heskestad's [40] correlation. McCaffrey divides the flame/plume into three regions:

$$\frac{\dot{m}_\mathrm{e}}{\dot{Q}} = \begin{cases} 0.011\left(\frac{z}{\dot{Q}^{2/5}}\right)^{0.566} & 0.00 \le \left(\frac{z}{\dot{Q}^{2/5}}\right) < 0.08 \\ 0.026\left(\frac{z}{\dot{Q}^{2/5}}\right)^{0.909} & 0.08 \le \left(\frac{z}{\dot{Q}^{2/5}}\right) < 0.20 \\ 0.124\left(\frac{z}{\dot{Q}^{2/5}}\right)^{1.895} & 0.20 \le \left(\frac{z}{\dot{Q}^{2/5}}\right) \end{cases} \tag{3.14}$$

Heskestad analyzed both his own data [40] and that of Zukoski [41] to develop the correlation

$$\dot{m}_\mathrm{e} = 0.071\,\dot{Q}_\mathrm{c}^{1/3}\,(z-z_0)^{5/3}\left(1+0.026\,\dot{Q}_\mathrm{c}^{2/3}\,(z-z_0)^{-5/3}\right) \tag{3.15}$$

where z_0 is a virtual origin for the fire plume defined as

$$z_0/D = -1.02 + 0.083\dot{Q}^{2/5}/D \tag{3.16}$$

which is based on the total heat release rate of the fire, $\dot{Q}$. Both correlations provide similar results in CFAST calculations.

In CFAST, there is a constraint on the mass entrainment rate because the plume can rise only so high for a given HRR. Early in a fire, the plume may not have sufficient energy to reach the compartment ceiling. Therefore, a limit is placed on the entrainment rate. For the plume to be able to penetrate the hot upper layer, the density of the gas in the plume must be less than the density of the gas in the upper layer. This implies that the upper layer temperature must be less than the plume temperature:

$$T_\mathrm{u} < T_\mathrm{p} \approx \frac{\dot{Q}_\mathrm{c} + \dot{m}_\mathrm{e}\,c_p\,T_\mathrm{l}}{\dot{m}_\mathrm{e}\,c_p} \tag{3.17}$$

Rearranging terms yields a limit on the mass entrainment:

$$\dot{m}_e < \frac{\dot{Q}_\mathrm{c}}{c_p(T_\mathrm{u} - T_\mathrm{l})} \tag{3.18}$$

3.4 Plume Centerline Temperature

CFAST includes an empirical correlation of plume centerline gas temperature based on the work of Baum and McCaffrey [42] with a modification by Evans [43] to account for the presence of a hot gas layer. The correlation gives the excess temperature as a function of height above a fire, z, for the flaming, intermittent, and plume regions:

$$\frac{\Delta T_\mathrm{p}}{T_\infty} = \begin{cases} 2.91 & 0.00 \le z/D^* < 1.32 \\ 3.81\,(z/D^*)^{-1} & 1.32 \le z/D^* < 3.30 \\ 8.41\,(z/D^*)^{-5/3} & 3.30 \le z/D^* \end{cases} \tag{3.19}$$

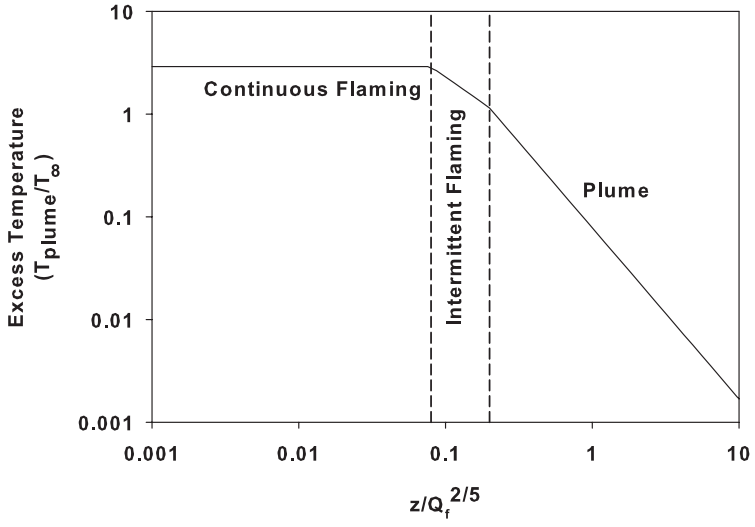

Figure 3.1: Excess plume centerline temperature from Baum and McCaffrey correlation.

where

$$D^* = \left(\frac{\dot{Q}}{\rho_\infty c_p T_\infty \sqrt{g}} \right)^{2/5} \tag{3.20}$$

Figure 3.1 shows the correlation. When a hot layer forms, the correlation must be modified since the plume now includes added enthalpy due to the entrainment of hot layer gases. Evans [43] defines a virtual source and heat release rate to extend the plume into the upper layer. Evans' method defines the strength and location of the substitute source with respect to the interface between the upper and lower layers by

$$Q^*_{I,2} = \left(\frac{1 + C_T {Q^*_{I,1}}^{2/3}}{\xi C_T} - \frac{1}{C_T} \right)^{3/2} \tag{3.21}$$

$$Z_{I,2} = \left(\frac{\xi Q^*_{I,1} C_T}{{Q^*_{I,2}}^{1/3} \left((\xi - 1)(\beta^2 + 1) + x1 C_T {Q^*_{I,2}}^{2/3} \right)} \right)^{2/5} Z_{I,1} \tag{3.22}$$

$$Q^*_{I,1} = \frac{Q_{f,C}}{\rho_\infty c_p T_\infty \sqrt{g} Z^{5/2}_{I,1}} \tag{3.23}$$

where $Z_{I,1}$ is the distance from the fire to the interface between the upper and lower gas layers, $Z_{I,2}$ is the distance from the virtual source to the layer interface, ξ is the ratio of the upper to lower layer temperature, β is an experimentally determined constant [41] ($\beta^2 = 0.913$), and $C_T = 9.115$. The effective source strength and distance between the virtual source and target position is given by

$$Q_{f,C,eff} = Q^*_{I,2} \rho_\infty c_{p\infty} T_\infty \sqrt{g} Z^{5/2}_{I,2} \tag{3.24}$$

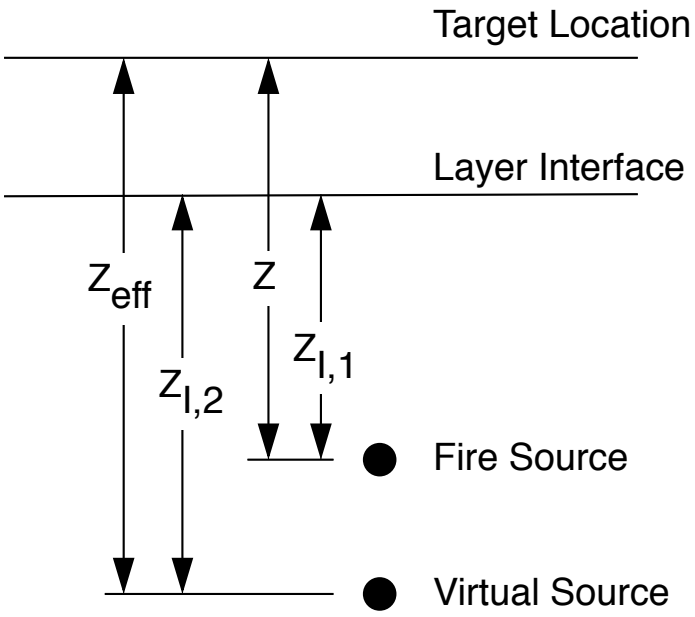

Figure 3.2: Geometry for plume centerline temperature calculation.

$$z_{eff} = z - Z_{I,1} + Z_{I,2} \tag{3.25}$$

(see Fig. 3.2). The new values of the fire source and target location are then used in the standard plume correlation where the ambient conditions are now those of the upper layer.

3.5 Flame Height

CFAST includes a calculation of average flame height based on the work of Heskestad [44]. Valid for a wide range of hydrocarbon and gaseous fuels, the correlation is given by

$$H = -1.02D + 0.235\left(\frac{Q_f}{1000}\right)^{2/5} \tag{3.26}$$

where H is the average flame height (m), D the diameter of the fire (m), and $\dot{Q}$ is the total heat release rate (kW). The mean flame height is defined as the distance from the fuel source to the top of the visible flame where the intermittency is 0.5. A flame intermittency of 0.5 means that the visible flame is above the mean 50 % of the time and below the mean 50 % of the time. This average flame height is included in the printed output from CFAST.

Chapter 4

Ventilation

Flow through vents is a dominant component of any fire model because it is sensitive to small changes in pressure and transfers the greatest amount of enthalpy on an instantaneous basis of all the source terms (except of course for the fire and plume). Its sensitivity to environmental changes arises through its dependence on the pressure difference between compartments which can change rapidly.

Flow through vents can be forced (mechanical) or natural (convective). CFAST models three types of vent flow, natural flow through vertical vents (such as doors or windows), natural flow through horizontal vents (such as ceiling holes or hatches) and forced flow throught fans. Horizontal flow is the flow which is normally thought of when discussing fires. Vertical flow is particularly important in two disparate situations: a ship, and the role of fire fighters doing roof venting.

Vent flow is determined using the pressure difference across a vent. Natural vent flow at a given elevation may be computed using Bernoulli's law by first computing the pressure difference at that elevation. The pressure on each side of the vent is computed using the pressure at the floor, the height of the floor and the density. Forced flow can occur through either vertical or horizontal vents. The differences are primarily the selection rules for the source of the gases or whether the resultant plume enters the lower or upper layer of each compartment.

Atmospheric pressure is about 100 000 Pa. Fires produce pressure changes from 1 Pa to 1 000 Pa and mechanical ventilation systems typically involve pressure differentials of about 1 Pa to 100 Pa. The pressure variables are solved to a higher accuracy than other solution variables because of the subtraction (with resulting loss of precision) needed to calculate vent flows from pressure differences.

Mass flow (in the remainder of this section, the term "flow" will be used to mean mass flow) is the dominant source term for the predictive equations because it fluctuates most rapidly and transfers the greatest amount of enthalpy on an instantaneous basis of all the source terms (except of course the fire). Also, it is most sensitive to changes in the environment. Horizontal flow encompasses flow through doors, windows and so on. Horizontal flow is discussed in section 3.4.3.1. Vertical flow occurs in ceiling vents. It is important in two separate situations: on a ship with open hatches and in house fires with roof venting. Vertical flow is discussed in section 3.4.3.2.

There is a special case of horizontal flow for long corridors. A corridor flow algorithm is incorporated to calculate the time delay from when a plume enters a compartment to when the effluent is available for flow into adjacent compartments.

Flow through vents can be modified, that is turned on or off. This applies to the three types

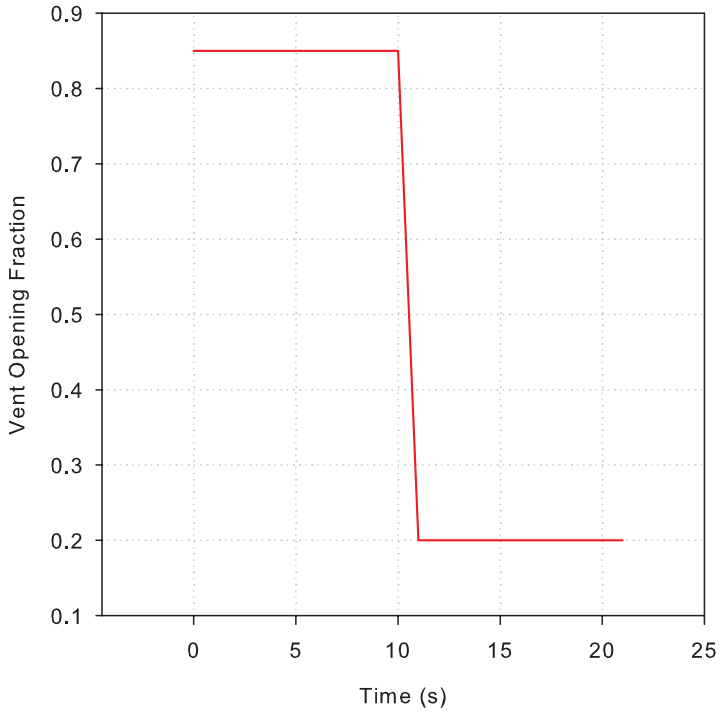

Figure 4.1: Vent opening size fraction as a function of time.

of vents discussed below, horizontal flow through vertical vents (HVENT), vertical flow through horizontal vents (VVENT) and forced flow (MVENT). For each key word, there is a an initial opening fraction which is reflected in the first region in Fig. 4.1. This initial opening fraction can be modified by by the EVENT key word to change the fraction. This change occurs over a transition time which defaults to one second. The final fraction is the third region depicted in Fig. 4.1. There can be only a single transition per vent.

4.0.1 Horizontal Flow Through Vertically-Oriented Vents (Doors and Windows)

Flow through normal vents such as windows and doors is governed by the pressure difference across a vent. A momentum equation for the zone boundaries is not solved directly. Instead momentum transfer at the zone boundaries is included by using an integrated form of Euler's equation, namely Bernoulli's solution for the velocity equation. This solution is augmented for restricted openings by using flow coefficients [45, 46] to allow for constriction from finite size doors. The flow (or orifice) coefficient is an empirical term which addresses the problem of constriction of velocity streamlines at an orifice.

Bernoulli's equation is the integral of the Euler equation and applies to general initial and final velocities and pressures. The implication of using this equation for a zone model is that the initial velocity in the doorway is the quantity sought, and the final velocity in the target compartment

vanishes. That is, the flow velocity vanishes where the final pressure is measured. Thus, the pressure at a stagnation point is used. This is consistent with the concept of uniform zones which are completely mixed and have no internal flow.

The mass flow through a region is found by first noting that the velocity of the flow at an elevation h is given by

$$v(h) = C\sqrt{\frac{2\Delta P(h)}{\rho}} \tag{4.1}$$

where C is the constriction (or flow) coefficient (taken to be 0.7 in CFAST [46]), ρ is the gas density on the source side, and $\Delta P(h)$ is the pressure across the interface at elevation h. At present we use a constant value for C for all gas temperatures.

The differential mass flow, $d\dot{m}(h)$, at elevation h through a region of width w and differential height dh is found using equation 4.1 after noting that $d\dot{m}(h) = v(h)\rho w dh$ to obtain

$$d\dot{m}(h) = C\sqrt{2\rho\Delta P(h)}w dh \tag{4.2}$$

The total mass flow rate through a slab is found by integrating $d\dot{m}(h)$ vertically over that slab. The simplest means to define the limits of integration is with neutral planes, that is the height at which flow reversal occurs, and physical boundaries such as sills and soffits. The mass flow equation can be integrated piecewise analytically and then summed by breaking the integral into intervals defined by flow reversal, a soffit, a sill, or a zone interface, .

The approach to calculating the flow field is of some interest. The flow calculations are performed as follows. The vent opening is partitioned into at most six slabs where each slab is bounded by a layer height, neutral plane, or vent boundary such as a soffit or sill. The most general case is illustrated in Fig. 4.2.

Let b and t denote the bottom and top slab elevations and P_b and P_t denote the cross-vent pressures at those elevations. Because of the way that slabs are defined, the two cross pressures P_b and P_t will have the same sign. The mass flow through the slab can then be computed by integrating equation 4.2 vertically from b to t to obtain

$$\begin{aligned}
\dot{m} &= \int_b^t d\dot{m}(h) && (4.3)\\
&= C\sqrt{2\rho}w\int_b^t \sqrt{\frac{|P_b(t-h)+P_t(h-b)|}{t-b}}dh && (4.4)\\
&= \frac{2}{3}C\sqrt{2\rho}w(t-b)\frac{|P_t|^{3/2}-|P_b|^{3/2}}{|P_t|-|P_b|} && (4.5)
\end{aligned}$$

after noting that

$$\int \sqrt{A+Bh}dh = \frac{2}{3B}(A+Bh)^{3/2} + \text{constant}$$

where $B = (|P_t| - |P_b|)/(t-b)$, $A + Bt = |P_t|$ and $A + Bb = |P_b|$. Equation 4.5 can be simplified to

$$\dot{m}_{io} = \frac{2}{3}C\sqrt{2\rho}A_{slab}\left(\frac{x^2+xy+y2}{x+y}\right) \tag{4.6}$$

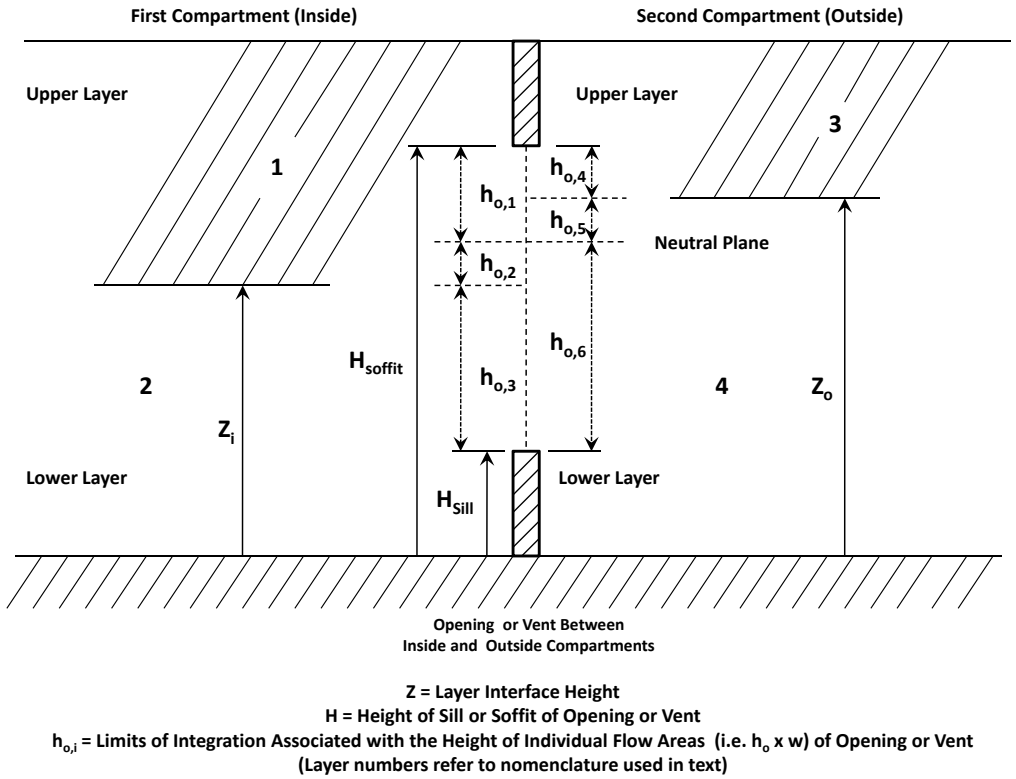

Figure 4.2: Geometry and notation for horizontal flow vents in a two-zone fire model.

where $x = \sqrt{|P_t|}$, $y = \sqrt{|P_b|}$, $A_{slab} = w(t-b)$ the cross-sectional area of the slab. The value of the density, ρ, is taken from the source compartment.

A mixing phenomenon occurs at vents which is similar to entrainment in plumes. As hot gases from one compartment leave that compartment and flow into an adjacent compartment a door jet can exist which is analogous to a normal plume. Mixing of this type occurs for $\dot{m}_{13} > 0$ as shown in Fig. 4.3. To calculate the entrainment ($\dot{m}_{43}$ in this example), once again we use a plume description consistent with the work of McCaffrey, but with an virtual origin. The estimate for the virtual origin is given by Cetegen et al. [47]. This is chosen so that the flow at the door opening would correspond to a plume with the heating for a equivalent doorway fire source (with respect to the lower layer) given by

$$Q_{f,eq} = c_p(T_1 - T_4)\dot{m}_{13} \tag{4.7}$$

where $Q_{f,eq}$ is the heat release rate of the doorway fire. The concept of the virtual origin is that the enthalpy flux from the virtual point source should equal the actual enthalpy flux in the door jet at the point of exit from the vent using the same prescription. Thus the entrainment is calculated the same way as was done for a normal plume. The reduced height of the plume, z_p, (in units of m/kW$^{2/5}$) is

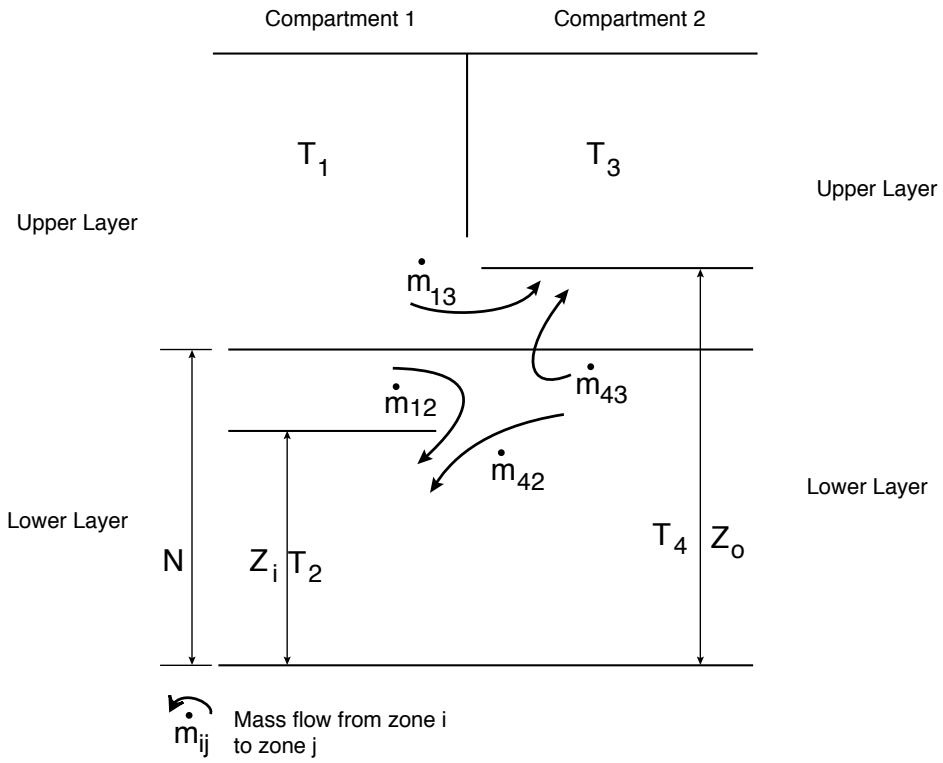

Figure 4.3: Flow patterns and layer number conventions for horizontal flow through a vertical vent.

$$z_p = \frac{z_{13}}{Q_{f,eq}^{2/5}} + v_p \tag{4.8}$$

where v_p the virtual point source, is defined by inverting the entrainment process to yield

$$\begin{aligned} v_P &= \left(\frac{8.10\dot{m}}{Q_{f,eq}}\right)^{0.528} && 0 < \left(\tfrac{\dot{m}}{Q_{f,eq}}\right) < 0.0061 \\ v_P &= \left(\frac{38.5\dot{m}}{Q_{f,eq}}\right)^{1.1001} && 0.0061 < \left(\tfrac{\dot{m}}{Q_{f,eq}}\right) \leq 0.026 \\ v_P &= \left(\frac{90.9\dot{m}}{Q_{f,eq}}\right)^{1.76} && \left(\tfrac{\dot{m}}{Q_{f,eq}}\right) > 0.026 \end{aligned} \tag{4.9}$$

Although outside of the normal range of validity of the plume model, a level of agreement with experiment is apparent (section 6 includes discussion of validation experiments for the plume model). Since a door jet forms a flat plume whereas a normal fire plume will be approximately circular, strong agreement is not expected.

The other type of mixing is much like an inverse plume and causes contamination of the lower layer. It occurs when there is flow of the type $\dot{m}_{42} > 0$. The shear flow causes vortex shedding into the lower layer and thus some of the particulates end up in the lower layer. The actual amount of mass or energy transferred is usually not large, but its effect can be large. For example, even

minute amounts of carbon can change the radiative properties of the gas layer, from negligible to something finite. It changes the rate of radiation absorption significantly and invalidates the simplification of an ambient temperature lower layer. This term is predicated on the Kelvin-Helmholz flow instability and requires shear flow between two separate fluids. The mixing is enhanced for greater density differences between the two layers. However, the amount of mixing has never been well characterized. Quintiere et al. [45] discuss this phenomena for the case of crib fires in a single room, but their correlation does not yield good agreement with experimental data in the general case [48]. In the CFAST model, it is assumed that the incoming cold plume behaves like the inverse of the usual door jet between adjacent hot layers; thus we have a descending plume. The same equations are used to calculate this inverse plume as are used for the upright door mixing, above. It is possible that the entrainment is overestimated in this case, since buoyancy, which is the driving force, is not nearly as strong as for the usually upright plume.

4.0.2 Vertical Flow Through Horizontally-Oriented Vents (Floor and Ceiling Vents)

Flow through a ceiling or floor vent can be somewhat more complicated than through door or window vents. The simplest form is uni-directional flow, driven solely by a pressure difference. This is analogous to flow in the horizontal direction driven by a piston effect of expanding gases. Once again, it can be calculated based on the Bernoulli equation, and presents little difficulty. However, in general we must deal with more complex situations that must be modeled in order to have a proper understanding of smoke movement. The first is an occurrence of puffing. When a fire exists in a compartment in which there is only one hole in the ceiling, the fire will burn until the oxygen has been depleted, pushing gas out the hole. Eventually the fire will die down. At this point ambient air will rush back in, enable combustion to increase, and the process will be repeated. Combustion is thus tightly coupled to the flow. The other case is exchange flow which occurs when the fluid configuration across the vent is unstable (such as a hotter gas layer underneath a cooler gas layer). Both of these pressure regimes require a calculation of the onset of the flow reversal mechanism.

Normally a non-zero cross vent pressure difference tends to drive unidirectional flow from the higher to the lower pressure side. An unstable fluid density configuration occurs when the pressure alone would dictate stable stratification, but the fluid densities are reversed. That is, the hotter gas is underneath the cooler gas. Flow induced by such an unstable fluid density configuration tends to lead to bi-directional flow, with the fluid in the lower compartment rising into the upper compartment. This situation might arise in a real fire if the room of origin suddenly had a hole punched in the ceiling. No pretense is made of being able to do this instability calculation analytically. Cooper's algorithm [49] is used for computing mass flow through ceiling and floor vents. It is based on correlations to model the unsteady component of the flow. What is surprising is that we can find a correlation at all for such a complex phenomenon. There are two components to the flow. The first is a net flow dictated by a pressure difference. The second is an exchange flow based on the relative densities of the gases. The overall flow is given by [49, 50, 51]

$$\dot{m} = Cf(\gamma,\varepsilon)\sqrt{\frac{\Delta P}{\bar{\rho}}}A_v \tag{4.10}$$

where $\gamma = c_p/c_v$ is the ratio of specific heats, $C = 0.68 + 0.17\varepsilon$, $\varepsilon = \frac{\Delta P}{P}$, and f us a weak function of both γ and ε [49]. In the situation where we have an instability, we use Cooper's correlations for the function f. The resulting exchange flow is given by

$$\dot{m}_{ex} = 0.1 \left(\frac{g \Delta \rho A_v^{5/2}}{\rho_{av}} \right) \left(1.0 - \frac{2 A_v^2 \Delta P}{S^2 g \Delta \rho D^5} \right) \tag{4.11}$$

where $D = 2\sqrt{A_v/\pi}$ and S is 0.754 for round or 0.942 for square openings, respectively [49]. Vertical flow through horizontal vents is governed by the VFLOW routines. VENTCF is the module which calculates the mass flow from one compartment to another. The values returned are $\dot{m}_{incoming}$ and $\dot{m}_{outgoing}$ through each vent. These terms are symmetric: the outgoing flow from compartment 1 to 2 is the same as incoming flow from compartment 2 to 1, though source and destination layers may be different.

The energy flux into a compartment is then determined by the relative size and temperature of the layers of the compartment from which the mass is flowing (incoming, u and l):

$$\dot{q}_{incoming} = c_p \dot{m}_u T_u + c_p \dot{m}_l T_l \tag{4.12}$$

$$\dot{m}_u = \dot{m}_{incoming} \frac{V_u}{V} \tag{4.13}$$

$$\dot{m}_l = \dot{m}_{incoming} \frac{V_l}{V} \tag{4.14}$$

The mass and energy are then deposited into the upper or lower layer of the receiving compartment based on the effective temperature of the incoming flow relative to the upper and lower layers of the receiving compartment. If the temperature of the incoming flow is higher than the temperature of the lower layer, then the flow is deposited into the upper layer. This is similar to the usual plume from a fire or a doorway jet. These rules are implemented in VFLOW.

4.0.3 Forced Flow

Forced flow in this version of CFAST is a supply (or exhaust) system based on constant flow through a opening/fan/opening triplet . These systems are commonly used in buildings for heating, ventilation, air conditioning, pressurization, and exhaust. Figure 4.4(a) shows smoke management by an exhaust fan at the top of an atrium, and Fig. 4.4(b) illustrates a kitchen exhaust. Cross ventilation, shown in Fig. 4.4(c), is occasionally used without heating or cooling. Generally systems that maintain comfort conditions have either one or two fans.

Further information about these systems is presented in Klote and Milke [52] and the American Society of Heating, Refrigerating and Air Conditioning Engineers (ASHRAE) [53].

This version of the model does not include duct work or variable fans. These equations are high-order, non-linear and in some cases ill-posed, which caused a great deal of difficulty in reaching a numerical solution.

The flow through mechanical vents can be filtered. Filtering affects particulates such as smoke and the trace species. Filtering can be turned on at any time. Effectiveness is from 0 % (no effect) to 100 % which completely blocks flow of these two species.

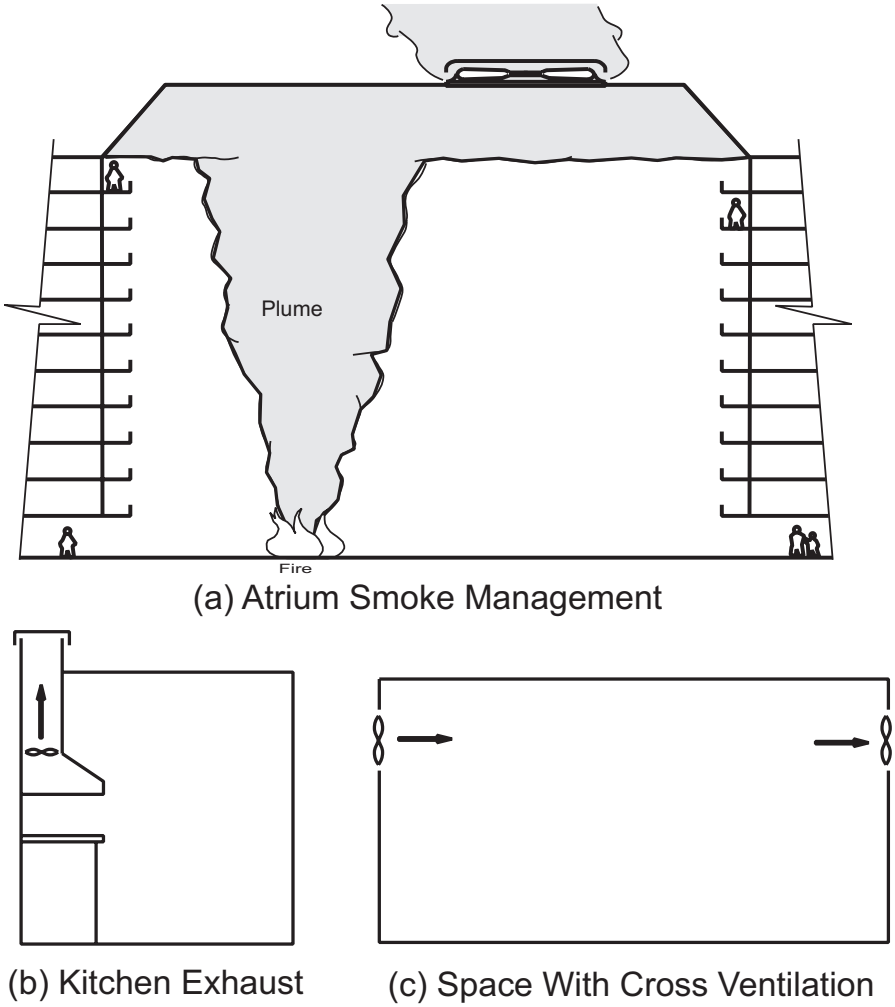

Figure 4.4: Some simple fan-duct systems.

Chapter 5

Heat Transfer

This section discusses radiation, convection and conduction, the three mechanisms by which heat is transferred between the gas layers and the enclosing compartment walls. This section also discusses heat transfer algorithms for calculating target temperatures.

Gas layers exchange energy with their surroundings via convective and radiative heat transfer. Different material properties can be used for the ceiling, floor, and walls of each compartment (although all the walls of a compartment must be the same). Additionally, CFAST allows each surface to be composed of up to three distinct layers. This allows the user to deal naturally with the actual building construction. Material thermophysical properties are assumed to be constant, although we know that they actually vary with temperature. The user should also recognize that the mechanical properties of some materials may change with temperature, but these effects are not modeled.

Radiative transfer occurs among the fire(s), gas layers and compartment surfaces (ceiling, walls and floor). This transfer is a function of the temperature differences and the emissivity of the gas layers as well as the compartment surfaces. Typical surface emissivity values only vary over a small range. For the gas layers, however, the emissivity is a function of the concentration of species which are strong radiators, predominately smoke particulates, carbon dioxide, and water. Thus errors in the species concentrations can give rise to errors in the distribution of enthalpy among the layers, which results in errors in temperatures, resulting in errors in the flows. This illustrates just how tightly coupled the predictions made by CFAST can be.

5.0.4 Radiation

Radiation heat transfer forms a significant portion of the energy balance in a zone fire model, especially in the fire room. Radiative heat transfer is computed from wall and gas temperatures, emisivities and fire heat release rates. To calculate the radiation absorbed in a zone, a heat balance must be done accounting for all surfaces that radiate to and absorb radiation from a zone.

A radiation heat transfer calculation can easily dominate the computational requirements of any fire model. Approximations are then required to perform these calculations in a time consistent with other zone fire model sources terms. For example, it is assumed that all zones and surfaces radiate and absorb like a gray body, that the fires radiate as point sources and that the plume does not radiate at all. Radiative heat transfer is approximated using a limited number of radiating wall surfaces, four in the fire room and two everywhere else. The use of these and other approximations

allows CFAST to perform the radiation computation in a reasonably efficient manner [55].

Modeling Assumptions: The following assumptions are made in order to simplify the radiation heat exchange model used in CFAST and to make its calculation tractable.

- Iso-thermal - Each gas layer and each wall segment is assumed to be at a uniform temperature.
- Equilibrium - The wall segments and gas layers are assumed to be in a quasi-steady state. In other words, the wall and gas layer temperatures are assumed to change slowly over the duration of the time step of the associated differential equation.
- Point Source Fires - The fire is assumed to radiate uniformly in all directions giving off a fraction, χ_R, of the total energy release rate. This radiation is assumed to originate from a single point. Radiation feedback to the fire and radiation from the plume is not modeled in the radiation exchange algorithm.
- Diffuse and gray surfaces - The radiation emitted is assumed to be diffuse and gray. In other words, the radiant fluxes emitted are independent of direction and wavelength. These assumptions allow us to infer that the emittance, ε, absorptance, α and reflectance, ρ, are related via $\varepsilon = \alpha = 1 - \rho$.
- Geometry - Rooms or compartments are assumed to be rectangular boxes. Each wall is either perpendicular or parallel to every other wall. Radiation transfer through vent openings is lost from the room.

4-Wall and 2-Wall Radiation Exchange: When computing wall temperatures, CFAST partitions a compartment into four parts; the ceiling, the floor, the wall segments above the layer interface and the wall segments below the layer interface. The radiation algorithm then computes a heat flux striking each wall segment using the surface temperature and emissivity.

The four wall algorithm used in CFAST for computing radiative heat exchange is based upon the equations developed in Siegel and Howell [56] which in turn is based on the work of Hottel [57]. Siegel and Howell model an enclosure with N wall segments and a homogeneous gas. A radiation algorithm for a two layer zone fire model requires treatment of an enclosure with two uniform gases. Hottel and Cohen [58] developed a method where the enclosure is divided into a number of wall and gas volume elements. An energy balance is written for each element. Each balance includes interactions with all other elements. Treatment of the fire and the interaction of the fire and gas layers with the walls is based upon the work of Yamada and Cooper [59]. They model fires as point heat sources radiating uniformly in all directions and use the Lambert-Beer law to model the interaction between heat emitting elements (fires, walls, gas layers) and the gas layers. By implementing a four wall rather than an N wall model, significant algorithmic speed increases are achieved. This is done by exploiting the simple structure and symmetry of the four wall problem.

The nomenclature used in this section follows that of Siegel and Howell [56]. The radiation exchange at the k'th surface is shown schematically in Fig. 5.1. For each wall segment k from 1 to N, a net heat flux, $\Delta\hat{q}''_k$, must be found such that the energy balance,

$$\sigma A_k \varepsilon_k T_k^4 + (1-\varepsilon_k) q_k^{in} = q_k^{in} + A_k \Delta q''_k \tag{5.1}$$

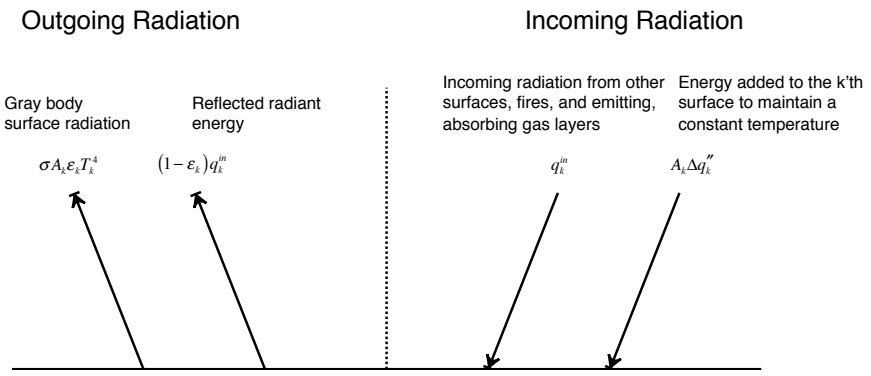

Figure 5.1: Radiation Exchange in a two-zone fire model.

at each wall segment k is satisfied, where σ is the Stefan-Boltzman constant, A_k is the area of the k'th wall segment , ε_k is the emissivity of the k'th wall segment, T_k is the temperature of the k'th wall segment and q_k^{in} is the energy arriving at the k'th wall segment from all other wall segments and heat sources.

Radiation exchange at each wall segment considers the emitted, reflected, incoming and net radiation terms. The unknown net radiative fluxes, $\Delta q_k''$, are found by solving the modified net radiation equation

$$\Delta \hat{q}_k'' - \sum_{j=1}^{N} \left(1-\varepsilon_j\right) \Delta \hat{q}_j'' F_{k-j} \tau_{j-k} = \sigma T_k^4 - \sum_{j=1}^{N} \left(\sigma T_k^4 F_{k-j} \tau_{k-j}\right) - \frac{c_k}{A_k} \tag{5.2}$$

where $\Delta \hat{q}_k'' = \Delta q_k / \varepsilon$, F_{k-j} is the configuration factor, τ is the transmittance and other terms are previously defined.

The walls can be modeled using two surfaces or four. The four wall model is necessary for fire rooms because the temperatures of the ceiling and upper walls differ significantly. The two wall model is used for compartments that contain no fires.

To simplify the comparison between the two and four wall segment models, assume that the emissivities of all wall segments are one and that the gas absorptivities are zero. Let the room dimensions be 4 m by 4 m by 4 m, the temperature of the floor and the lower and upper walls be 300 K, and the ceiling temperature vary from 300 K to 600 K. Figure 5.2 shows a plot of the heat flux to the ceiling and upper wall as a function of the ceiling temperature [55, 60]. The two wall model predicts that the extended ceiling (a surface formed by combining the ceiling and upper wall into one wall segment) cools, while the four wall model predicts that the ceiling cools and the upper wall warms. The four-wall model better accounts for temperature differences that may exist between the ceiling and upper wall (or floor and lower wall) by allowing heat transfer to occur between the ceiling and upper wall. This problem is not as significant in compartments where a fire is not present.

Reference [55] documents how to minimize the work required to compute the 16 configuration factors, F_{k-j}, required in a 4 wall model.

Configuration Factors: A configuration factor between two finite areas denoted F_{1-2} is the

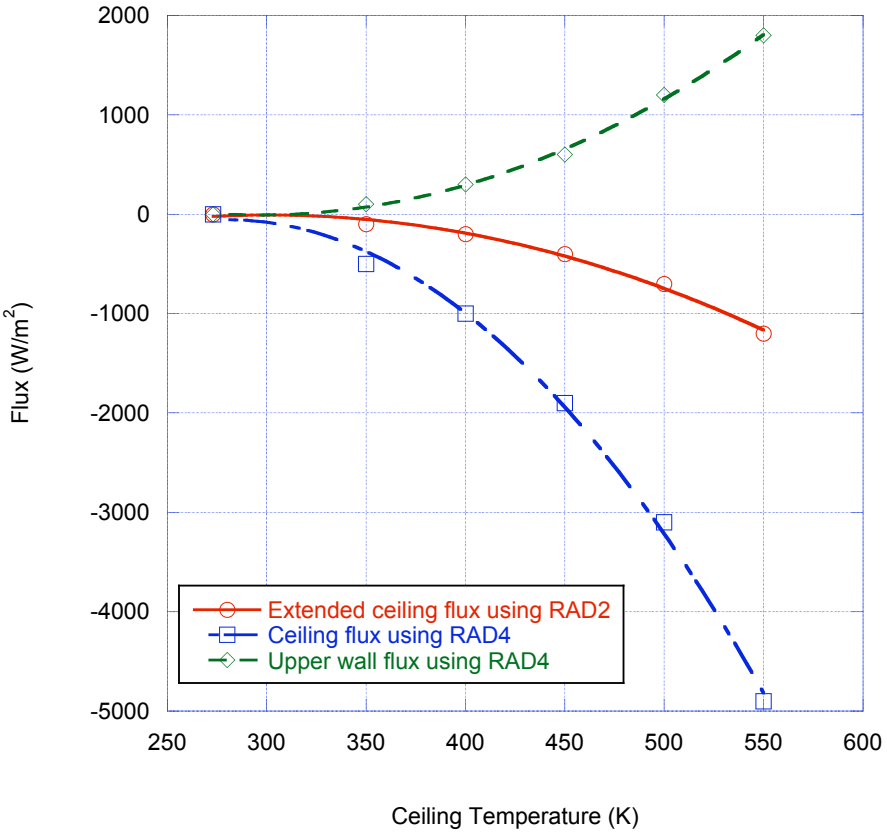

Figure 5.2: An example of the calculated two-wall (RAD2) and four-wall (RAD4) contributions to radiation exchange on a ceiling and wall surface.

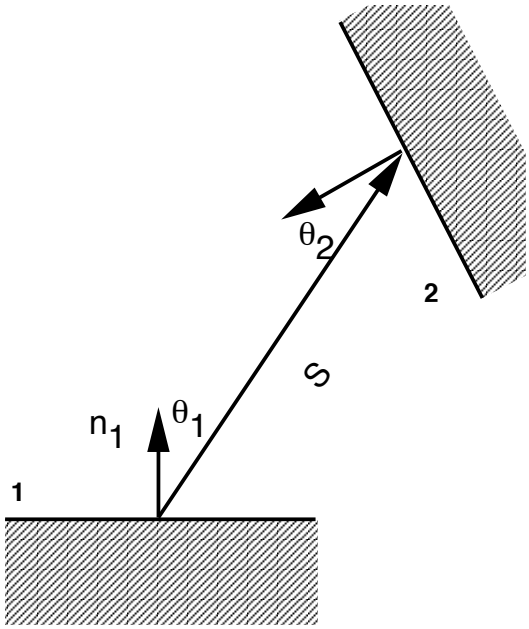

Figure 5.3: Setup for a configuration factor calculation between two arbitrarily oriented finite areas.

fraction of radiant energy given off by surface 1 that is intercepted by surface 2 and is given by

$$F_{1-2} = \frac{1}{A_1}\int_{A_1}\int_{A_2}\frac{\cos\theta_1\theta_2}{\pi L^2}dA_2 dA_1 \tag{5.3}$$

where L is the distance along the line of integration, θ_1 and θ_2 are the angles for surface 1 and 2 between the respective normal vectors and the line of integration, and A_1 and A_2 are the areas of the two surfaces. These terms are illustrated in Fig. 5.3. When the surfaces A_1 and A_2 are far apart relative to their surface area, eq (5.3) can be approximated by assuming that θ_1, $theta_2$ and L are constant over the region of integration to obtain

$$F_{1-2} = \frac{\cos\theta_1\theta_2}{\pi L^2}A_2 \tag{5.4}$$

Transmittance and Absorptance: The transmittance of a gas volume is the fraction of radiant energy that will pass through it unimpeded and is given by

$$\tau(L) = e^{-\alpha L} \tag{5.5}$$

where α is the absorptance of the gas volume and L is a characteristic path length.

The absorptance, α, of a gas volume is the fraction of radiant energy absorbed by that volume. For a gray gas, $\alpha + \tau = 1$.

Calculating absorption for broad band gas layer radiation: In general, the transmittance and absorptance are a function of wavelength. This is an important factor to consider for the major gaseous products (CO_2 and H_2O); however soot has a continuous absorption spectrum which

allows the transmittance and absorptance to be approximated as "gray" [56] across the entire spectrum.

The gas absorptance, α_G, is due to the combination of the CO_2 and H_2O and is given by

$$\alpha_G = \alpha_{H_2O} + \alpha_{CO} - C \tag{5.6}$$

where C is a correction for band overlap. For typical fire conditions, the overlap amounts to about half of the CO_2 absorptance [61] so the gas transmittance is approximated by

$$\tau_G = 1 - \alpha_{H_2O} - 0.5\alpha_{CO_2} \tag{5.7}$$

The total transmittance of a gas-soot mixture is the product of the gas and soot transmittances, $\tau_T = \tau_S \tau_G$ so that

$$\tau_T = e^{-al}(1 - \alpha_{H_2O} - 0.5\alpha_{CO_2}) \tag{5.8}$$

In the optically thin limit the absorption coefficient, a, may be replaced by the Planck mean absorption coefficient and in the optically thick limit, it may be replaced by the Rosseland mean absorption coefficient. For the entire range of optical thicknesses, Tien et al. [61] report that a reasonable approximation is $\alpha = k f_v T$ where k is a constant that depends on the optical properties of the soot particles, f_v is the soot volume fraction and T is the soot temperature in Kelvin. Values of a, have been found to be about constant for a wide range of fuels [62]. The soot volume fraction, f_v, is calculated from the soot mass, soot density and layer volume. The soot is assumed to be in thermal equilibrium with the gas layer.

Edwards' absorptance data for H_2O and CO_2 are reported [63] as log(emissivity) versus log(pressure-pathlength), with log(gas concentration) as a parameter. For each gas, these data were incorporated into a look-up table, implemented as a two-dimensional array of log(emissivity) values, with indices based on temperature and gas concentration. It is assumed that absorptance and emittance are equivalent for the gaseous species as well as for soot.

An effective path length (mean beam length, L) treats an emitting volume as if it were a hemisphere of a radius such that the flux impinging on the center of the circular base is equal to the average boundary flux produced by the real volume. The value of this radius is approximated as [62, 64] $L = c4V/A$ where L is the mean beam length in meters, c is a constant (approximately 0.9, for typical geometries), V is the emitting gas volume m^3 and A is the surface area (m^2) of the gas volume. The volume and surface area are calculated from the dimensions of the layer.

For each gas, the log(absorptance) is estimated from the look-up table for that gas by interpolating both the log(temperature) and log(concentration) domains. In the event that the required absorptance lies outside the temperature or concentration range of the look-up table, the nearest acceptable value is returned. Error flags are also returned, indicating whether each parameter was in or out of range and, in the latter case, whether it was high or low. This entire process is carried out for both CO_2 and H_2O.

5.0.5 Computing Target Heat Flux and Temperature

The calculation of the radiative heat flux to a target is similar to the radiative heat transfer calculation discussed previously. The main difference is that CFAST does not compute feedback from

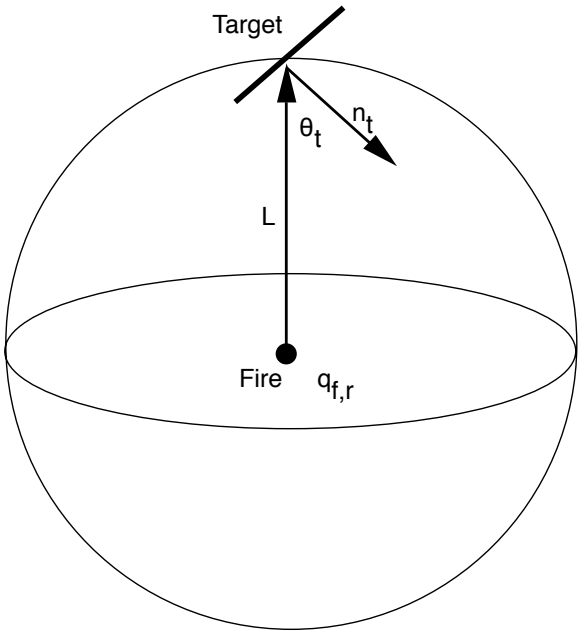

Figure 5.4: Radiative heat transfer from a point source fire to a target.

the target to the wall surfaces or gas layers. The target is simply a probe or sensor not interacting with the modeled environment.

The net flux striking a target can be used as a boundary condition in order to compute the temperature of the target. If the target is thin, then its temperature quickly rises to a level where the heat flux to and from the target are in equilibrium.

There are four components of heat flux to a target: fires, walls (including the ceiling and floor), gas layer radiation and gas layer convection.

Heat Flux from a Fire to a Target: Figure 5.4 illustrates terms used to compute heat flux from a fire to a target. Let n_t be a unit vector perpendicular to the target and θ_t be the angle between the vectors $\overline{L}$ and n_t.

Using the definition that $q_{f,r}$ is the radiative portion of the energy release rate of the fire, then the heat flux on a sphere of radius L due to this fire is $q_{f,r}/\left(4\pi L^2\right)$. Correcting for the orientation of the target and accounting for heat transfer through the gas layers, the heat flux to the target is

$$q''_{f,r} = \frac{q_{f,r}}{4\pi L^2}\cos(\theta_t)\tau_U(L_U)\tau_L(L_L) = -q_{f,r}\frac{n_t\overline{L}}{4\pi L^3}\tau_U(L_U)\tau_L(L_L) \tag{5.9}$$

Radiative Heat Flux from a Wall Segment to a Target: Figure 5.5 illustrates terms used to compute heat flux from a wall segment to a target. The flux, $q''_{w,t}$, from a wall segment to a target can then be computed using

$$q''_{w,t} = \frac{A_w q''_{w,out} F_{w-t}}{A_t}\tau_U(L_U)\tau_L(L_L) \tag{5.10}$$

where $q''_{w,t}$ is the flux leaving the wall segment, A_w, A_t are the areas of the wall segment and target respectively, F_{w-t} is the fraction of radiant energy given off by the wall segment that is intercepted

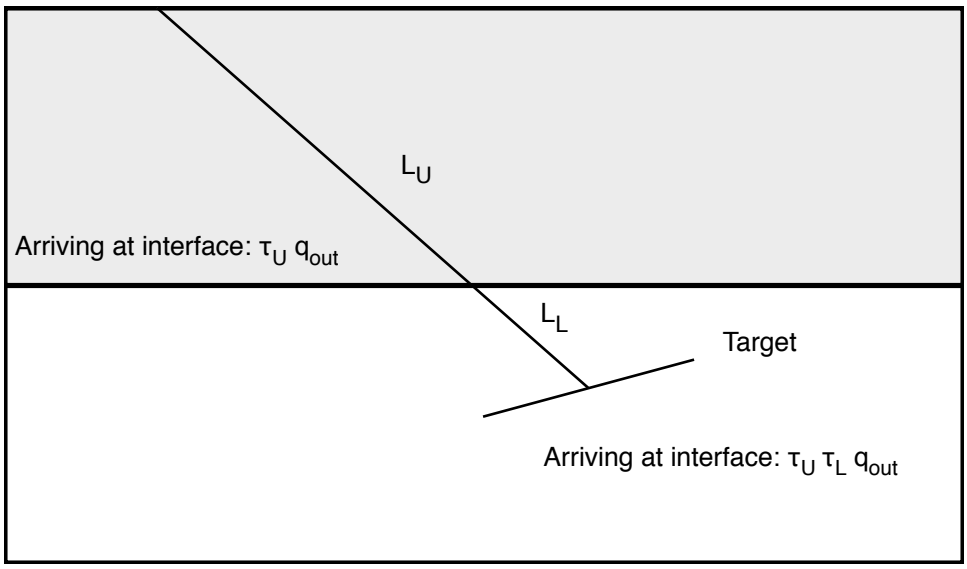

Figure 5.5: Radiative heat transfer from the upper and lower layer gas to a target in the lower layer.

by the target (i.e., a configuration factor) and $\tau_U(L_U)$ and $\tau_L(L_L)$ are defined as before. Equation (5.10) can be simplified using the symmetry relation $A_w F_{w-t} = A_t F_{t-w}$ to obtain

$$q''_{w,t} = q''_{w,out} F_{t-w} \tau_U(L_U) \tau_L(L_L) \tag{5.11}$$

where

$$q''_{w,out} = \sigma T_w^4 - (1-\varepsilon_w)\frac{\Delta q''_w}{\varepsilon_w}, \tag{5.12}$$

T_w is the temperature of the wall segment, ε_w is the emissivity of the wall segment and $\Delta q''_w$ is the net flux striking the wall segment.

Radiation from the Gas Layer to the Target: Figure 5.5 illustrates the setup for calculating the heat flux from the gas layers to the target. The upper and lower gas layers in a room contribute to the heat flux striking the target if the layer absorptances are non-zero.

Let $q''_{w,t,gas}$ denote the flux striking the target due to the gas g in the direction of wall segment w. Then

$$q''_{w,t,gas} = \begin{cases} \sigma F_{t-w}\left(T_L^4 \alpha_L \tau_U + T_U^4 \alpha_U\right) & w \text{ is in the lower layer} \\ \sigma F_{t-w}\left(T_U^4 \alpha_U \tau_L + T_L^4 \alpha_L\right) & w \text{ is in the upper layer} \end{cases} \tag{5.13}$$

The total target flux due to the gas (upper or lower layer) is obtained by summing eq (5.13 over each wall segment or

$$q''_{g,t} = \sum_w = q''_{w,t,gas} \tag{5.14}$$

Computing the Steady State Target Temperature: The steady state target temperature, T_t can be found by solving an energy balance on the target; namely

$$\varepsilon_t \sigma T_t^4 = \varepsilon_t q_{r,in} + h(T_g - T_t) \tag{5.15}$$

Note that the local gas temperature, T_g, in the convection calculation, $h(T_g - T_t)$, is taken to be either the upper layer temperature if the target is located in the upper layer, the lower layer temperature if the target is located in the lower layer, or the plume centerline temperature if the target is located directly above a fire source.

Let $f(T_t)$ be the difference between the left and right hand side of equation (5.15). Then this equation may be solved using the Newton iteration

$$T_{new} = T_{old} - \frac{f(T_{old})}{f'(T_{old})} \tag{5.16}$$

Equation (5.16) is iterated until the difference $T_{new} - T_{old}$ is sufficiently small.

Computing the Transient Rectangular Target Temperature: A transient target temperature may be computed using two different methods depending on whether the target is assumed to be thin or thick. A thin target is presumed to have a constant interior temperature profile. A differential equation model may then be used to estimate the temperature rise (or fall) based upon the thermal properties of the target and the heat flux striking the front and back sides; namely

$$c\rho V \frac{dT}{dt} = A(q''_f + q''_b) \tag{5.17}$$

where c, ρ and V are the the specific heat, density and volume of the target, A is the cross-sectional area of the target and the two q'' terms are the heat flux (due to all sources) striking the front and back sides of the target.

Equation (5.17) may be solved implicitly or explicitly. When solved implicitly, the target temperature is added to the set of solution variables and equation (5.17) is added to the equation set solved by DASSL. When solved explicitly, equation (5.17) is solved as a stand-alone equation advancing the target temperature in time.

If the target is thick then it is presumed that the temperature profile within the target varies as a function of depth and therefore a partial differential equation model must be used to estimate the changing profile; namely the heat equation

$$\frac{\partial T}{\partial t} = \frac{k}{\rho C} \frac{\partial^2 T}{\partial x^2} \tag{5.18}$$

where k, ρ and C are the thermal conductivity, density and heat capasity of the target. As with the standard heat conduction model discussed later, the target heat conduction model in CFAST couples the solid to the gas phase using the relation

$$q'' = -k \frac{dT}{dx} \tag{5.19}$$

where q'' is the heat flux striking the target (again due to all sources). This equation is the statment that the flux striking the target must be consistent with the temperature gradient at the surface.

Equation (5.18) may be solved implicitly or explicitly. When solved implicitly, the target temperature is added to the set of solution variables and equation (5.19) (not equation (5.18) is

added to the equation set solved by DASSL. When solved explicitly, equation (5.18) is solved as a stand-alone equation advancing the temperature profile in time.

Computing Transient Cable Target Heat Transfer:

This section describes a CFAST implementation of a model for predicting electrical cable failure first proposed by Andersson and Van Hees Ref. [65] and later implemented by McGrattan in FDS [66] . This model uses a simple one-dimensional heat transfer calculation, under the assumption that the cable can be treated as a homogenous cylinder [65].

The heat flux used to generate the heat transfer in the cable is provided by CFAST which models the thermal environment of the compartment where the cable is located. In most realistic fire scenarios, the heat flux to the cable is not axially-symmetric. CFAST therefore uses the maximum heat flux value when modeling cable failure.

1D heat transfer may be computed within a cylindrically symmetric target by splitting it into N concentric control volumes and performing an energy balance on each. The energy balance for the i'th control volume for $i = 1 \cdots N-1$, is

$$c\rho V_i \Delta T_i = (\dot{q}_i - \dot{q}_{i-1})\Delta t \tag{5.20}$$

where $c\rho V_i \Delta T_i$ represents the change in internal energy and $(\dot{q}_i - \dot{q}_{i-1})\Delta t$ represents the net heat flow across the control volume's inner and outer boundary surface over a Δt time period. The energy balance for the outermost or N'th control volume is similar

$$c\rho V_N \Delta T_N = (\dot{q}''_{ext} A_N - \dot{q}_{N-1})\Delta t \tag{5.21}$$

with $\dot{q}''_{ext} A_N$ used to specify a boundary condition, the combined net radiative and convective heat flux incident on the the cylindrical target's outer surface.

As illustrated in Figure 5.6, the i'th control volume has volume V_i, temperature T_i and heat flow at the inner and outer boundaries of $\dot{q}_{i-1}$ and $\dot{q}_i$ respectively. The i'th control volume has length L and inner and outer radius r_{i-1} and r_i where $r_i = i\Delta r$ and $\Delta r = R/N$. The density and specific heat of material in all control volumes is c and ρ.

The right hand sides of equations 5.20 and (5.21) may be expressed in terms of temperature using Fourier's law and noting that $\dot{q}_i = \dot{q}''_i A_i$ to obtain

$$c\rho V_i \Delta T_i = (\dot{q}''_i A_i - \dot{q}''_{i-1} A_{i-1})\Delta t = \left[k \left(\frac{T_{i+1} - T_i}{\Delta r} \right) A_i - k \left(\frac{T_i - T_{i-1}}{\Delta r} \right) A_{i-1} \right] \tag{5.22}$$

The volume of the i'th control volume is given by

$$V_i \;=\; \pi(r_i^2 - r_{i-1}^2)L = \pi\Delta r(r_i + r_{i-1})L = 2\pi\Delta r(i - 0.5)L$$

The area, A_i, of the outer boundary surface of the i'th control volume is given by

$$A_i = 2\pi r_i L = 2\pi\Delta r i L$$

Using the ratio $A_i/V_i = i/(\Delta r(i-0.5))$ and $\Delta T_i = T_i^{n+1} - T_i^n$, equation (5.22) may be simplified to

$$T_i^{n+1} - T_i^n \;=\; \frac{\Delta t}{\rho c} \left[\left(\frac{T_{i+1}^{n+1} - T_i^{n+1}}{\Delta r} \right) \frac{A_i}{V_i} - \left(\frac{T_i^{n+1} - T_{i-1}^{n+1}}{\Delta r} \right) \left(\frac{A_{i-1}}{V_i} \right) \right]$$

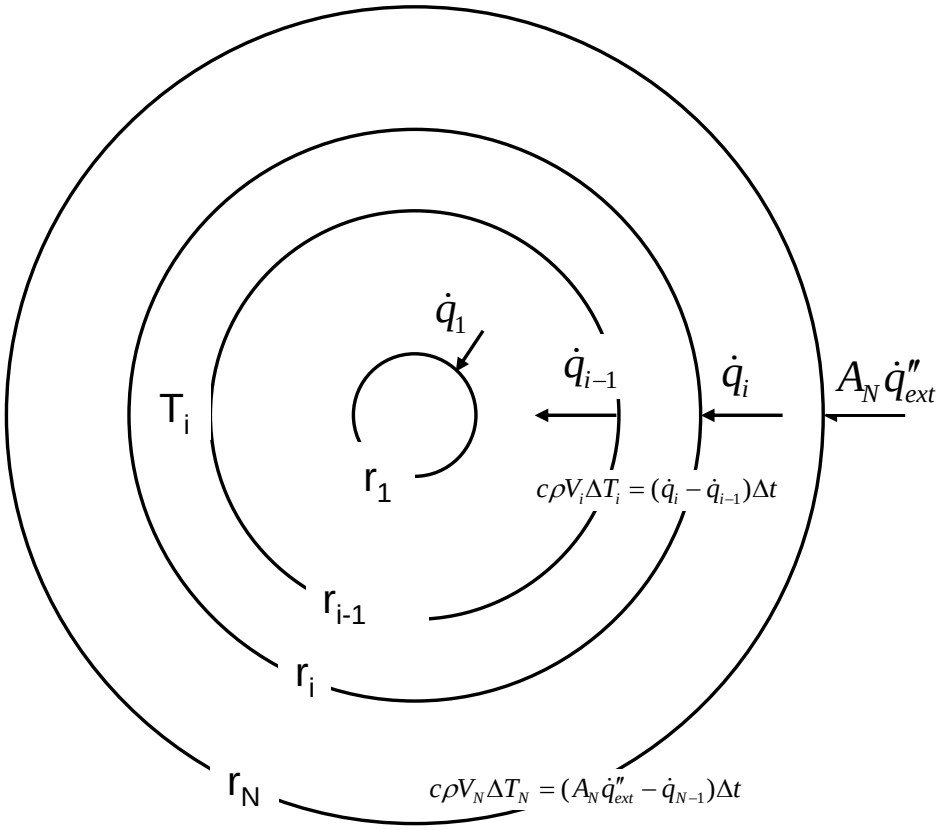

Figure 5.6: Schematic of a control volume for heat transfer in a cylindrical object.

$$\begin{aligned} &= \frac{\Delta t}{\Delta r^2}\frac{k}{\rho c}\left[\left(T_{i+1}^{n+1}-T_i^{n+1}\right)\left(\frac{i}{i-0.5}\right)-\left(T_i^{n+1}-T_{i-1}^{n+1}\right)\left(\frac{i-1}{i-0.5}\right)\right] \\ &= \frac{\alpha\Delta t}{\Delta r^2(i-0.5)}\left[\left(T_{i+1}^{n+1}-T_i^{n+1}\right)i-\left(T_i^{n+1}-T_{i-1}^{n+1}\right)(i-1)\right] \end{aligned} \tag{5.23}$$

where $\alpha - k/(\rho c)$. Defining C_i and D_i as

$$\begin{aligned} C_i &= \frac{\alpha\Delta t}{\Delta r^2}\left(\frac{i-1}{i-0.5}\right) \\ D_i &= \frac{\alpha\Delta t}{\Delta r^2}\left(\frac{i}{i-0.5}\right), \end{aligned}$$

noting that $C_i + D_i = 2\frac{\alpha\Delta t}{\Delta r^2}$ for $i = 1\cdots N-1$ and substituting into (5.23) results in

$$-C_i T_{i-1}^{n+1} + (1+2\frac{\alpha\Delta t}{\Delta r^2})T_i^{n+1} - D_i T_{i+1}^{n+1} = T_i^n \tag{5.24}$$

The energy balance for the N'th (outermost) control volume may be obtained by substituting $\Delta r q''_{ext}/k$ for $T_{i+1}^{n+1} - T_i^{n+1}$ in equation (5.23) to obtain

$$T_N^{n+1} - T_N^n = \frac{\alpha\Delta t}{\Delta r^2(N-0.5)}\left[\frac{\Delta r \dot{q}''_{ext}}{k}N - (T_N^{n+1} - T_{N-1}^{n+1})(N-1)\right]$$

then substituting C_N and D_N and simplifying to obtain

$$-C_N T_{N-1}^{n+1} + (1+C_N) T_N^{n+1} = T_N^n + D_N \frac{\Delta r}{k} q''_{ext} \tag{5.25}$$

Equations (5.24) and (5.25) represent a tri-diagonal linear system of equations which when written in matrix form are given by

$$\begin{pmatrix} 1+D_1 & -D_1 & & & & & \\ & \ddots & & & & & \\ & & -C_i & 1+2\frac{\alpha\Delta t}{\Delta r^2} & D_i & & \\ & & & & \ddots & & \\ & & & & & -C_N & 1+C_N \end{pmatrix} \begin{pmatrix} T_1^{n+1} \\ T_2^{n+1} \\ \vdots \\ T_{i-1}^{n+1} \\ T_i^{n+1} \\ T_{i+1}^{n+1} \\ \vdots \\ T_{N-1}^{n+1} \\ T_N^{n+1} \end{pmatrix} = \begin{pmatrix} T_1^n \\ T_2^n \\ \vdots \\ T_{i-1}^n \\ T_i^n \\ T_{i+1}^n \\ \vdots \\ T_{N-1}^n \\ T_N^n + D_N \frac{\Delta r}{k} \dot{q}''_{ext} \end{pmatrix} \tag{5.26}$$

Equation (5.26) is then used to advance the cable's temperature profile by Δt.

5.0.6 Convection

In general, convective heat transfer, q'', across a surface of area A_S, is defined as

$$q'' = hA_S(T_g - T_s) \tag{5.27}$$

The convective heat transfer coefficient, h, is a function of the gas properties, temperature, and velocity. The Nusselt number is defined as $Nu_L = hL/k$, which for natural convection is related to the Rayleigh number, $Ra_L = g\beta(T_s - T_g)L^3/\nu\alpha$ where L is a characteristic length of the geometry, g is the gravitational constant (m/s^2), k is the thermal conductivity (W/m^2 K), β is a volumetric expansion coefficient (K^{-1}), T_s and T_g are the temperatures of the surface and gas, respectively (K), ν is the kinematic viscosity (m^2/s), and α is the thermal diffusivity (m^2/s). All properties are evaluated at the film temperature, $T_f = (T_s + T_g)/2$. The typical correlations applicable to the problem at hand are available in the literature [67]. The table below gives the correlations used in CFAST.

The Prandtl number, Pr, is the ratio of the kinematic viscosity and the thermal diffusivity. The thermal diffusivity, α, and thermal conductivity, k, of air are defined as a function of the film temperature from data in reference [67] as

$$\alpha = 1.0x10^{-9} T_f^{7/4} \tag{5.28}$$

$$k = \frac{0.0209 + 2.33x10^{-5} T_f}{1 - 0.000267 T_f} \tag{5.29}$$

Geometry	Correlation	Restrictions
Walls	$Nu_L = \left(0.825 + \frac{0.387Ra_L^{1/6}}{\left(1+(0.492/Pr)^{9/16}\right)^{8/27}}\right)^2$ $= 0.12$	none
Ceilings and floors (hot surface up or cold surface down	$Nu_L = 0.13Ra_L^{1/3}$	$2x10^8 \leq Ra_L \leq 10^{11}$
Ceilings and floors (cold surface up or hot surface down	$Nu_L = 0.16Ra_L^{1/3}$	$2x10^8 \leq Ra_L \leq 10^{10}$

5.0.7 Conduction

Procedures for solving 1-d heat conduction problems are well known, (e.g., backward difference (fully implicit), forward difference (fully explicit) or Crank-Nicolson [68]). A finite difference approach using a non-uniform spatial mesh is used to advance the wall temperature solution. The heat equation is discretized using a second order central difference for the spatial derivative and a backward differences for the time derivative. The resulting tri-diagonal system of equations is then solved to advance the temperature solution to time $t + \Delta t$. This process is repeated , using the work of Moss and Forney [69], until the heat flux striking the wall (calculated from the convection and radiation algorithms) is consistent with the flux conducted into the wall calculated via Fourier's law

$$q'' = -k\frac{dT}{dx} \tag{5.30}$$

where k is the thermal conductivity. This solution strategy requires a differential algebraic equation (DAE) solver that can simultaneously solve both differential and algebraic equations. With this method, only one or two extra equations are required per wall segment (two if both the interior and exterior wall segment surface temperatures are computed). This solution strategy is more efficient than the method of lines since fewer equations need to be solved. Wall segment temperature profiles, however, still have to be stored so there is no decrease in storage requirements. Conduction is then coupled to the room conditions by temperatures supplied at the interior boundary by the differential equation solver. The exterior boundary conditions are modeled as surfaces that exchange heat with an ambient surroundings for both convection and radiation.

A non-uniform mesh scheme was chosen to allow grid points in the calculation to cluster near the interior and exterior wall segment surfaces. This is where the temperature gradients are the steepest. A breakpoint x_b was defined by $x_b = MIN(x_p, W/2)$ where W is the wall thickness and $x_p = 2\sqrt{\alpha t_{final}}erfc^{-1}(.05)$ and $erfc^{-1}$ denotes the inverse of the complementary error function. The value x_p is the location in a semi-infinite wall where the temperature rise is 5 % after t_{final} seconds and is sometimes called the penetration depth. Eighty percent of the grid points were placed on the interior side of x_b and the remaining 20 % were placed on the exterior side.

To illustrate the method, consider a one room case with one active wall. There are four gas equations (pressure, upper layer volume, upper layer temperature, and lower layer temperature)

and one wall temperature equation. Implementation of the gradient matching method requires that storage be allocated for the temperature profile at the previous time, t, and at the next time, $t + \Delta t$. Given the profile at time t and values for the five unknowns at time $t + \Delta t$ (initial guess by the solver), the temperature profile is advanced from time t to time $t + \Delta t$. The temperature profile gradient at $x = 0$ is computed followed by the residuals for the five equations. The DAE solver adjusts the solution variables and the time step until the residuals for all the equations are below an error tolerance. Once the solver has completed the step, the array storing the temperature profile for the previous time is updated, and the DAE solver is ready to take its next step.

5.0.8 Inter-compartment Heat Transfer

Heat transfer between vertically connected compartments is modeled by merging the connected surfaces for the ceiling and floor compartments or for the connected horizontal compartments. A heat conduction problem is solved for the merged walls using a temperature boundary condition for both the near and far wall. As before, temperatures are determined by the DAE solver so that the heat flux striking the wall surface (both interior and exterior) is consistent with the temperature gradient at that surface.

For horizontal heat transfer between compartments, the connections may be between partial wall surfaces, expressed as a fraction of the wall surface. CFAST first estimates conduction fractions analogous to radiative configuration factors. For example, if only one half of the rear wall in one compartment is adjacent to the front wall in a second compartment, the conduction fraction between the two compartments is 1/2. Once these fractions are determined, an average flux, q''_{avg}, is calculated using

$$q''_{avg} = \sum_{walls} F_{ij} q''_{wall_j} \tag{5.31}$$

where F_{ij} is the fraction of flux from wall i that contributes to wall j, q''_{wall_j} is the flux striking wall j.

5.0.9 Ceiling Jet

Relatively early in the development of a fire, fire-driven ceiling jets and gas-to-ceiling convective heat transfer can play a significant role in room-to-room smoke spread and in the response of near-ceiling mounted detection hardware. Cooper [70] details a model and computer algorithm to predict the instantaneous rate of convective heat transfer from fire plume gases to the overhead ceiling surface in a room of fire origin. The room is assumed to be a rectangular parallelepiped and, at times of interest, ceiling temperatures are simulated as being uniform. Also presented is an estimate of the convective heat transfer due to ceiling-jet driven wall flows. The effect on the heat transfer of the location of the fire within the room is taken into account. This algorithm has been incorporated into the CFAST model. In this section, we provide an overview of the model. Complete details are available in reference [[70].

A schematic of a fire, fire plume, and ceiling jet is shown in Fig. 5.7. The buoyant fire plume rises from the height Z_{fire} toward the ceiling. When the fire is below the layer interface, its mass and enthalpy flow are assumed to be deposited into the upper layer at height Z_{layer}. Having penetrated the interface, a portion of the plume typically continues to rise toward the ceiling. As it

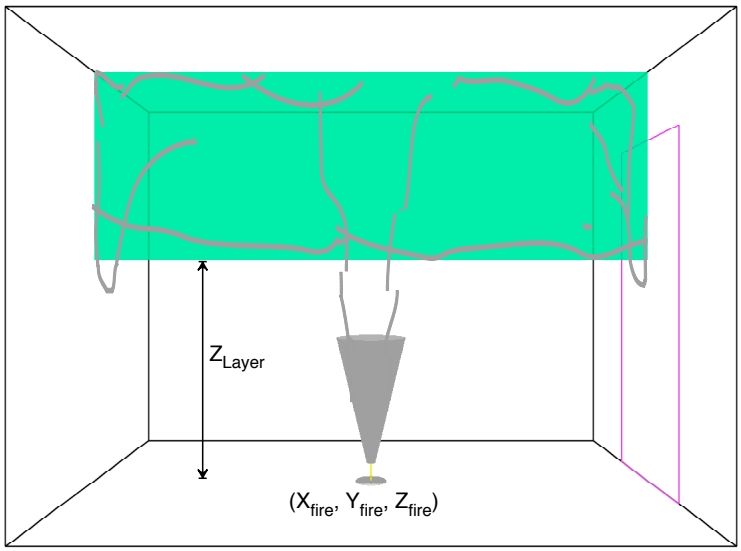

Figure 5.7: Convective heat transfer to ceiling and wall surfaces via the ceiling jet.

impinges on the ceiling surface, the plume gases turn and form a relatively high temperature, high velocity, turbulent ceiling jet which flows radially outward along the ceiling and transfers heat to the relatively cool ceiling surface. The convective heat transfer rate is a strong function of the radial distance from the point of impingement, reducing rapidly with increasing radius. Eventually, the relatively high temperature ceiling jet is blocked by the relatively cool wall surfaces [71]. The ceiling jet then turns downward and outward in a complicated flow along the vertical wall surfaces [72, 73] . The descent of the wall flows and the heat transfer from them are eventually stopped by upward buoyant forces. They are then buoyed back upward and mix with the upper layer.

The average convective heat transfer from the ceiling jet gases to the ceiling surface, Q_{ceil}, can be expressed in integral form as

$$Q_{ceil} = \int_0^{X_{wall}} \int_0^{Y_{wall}} q''_{ceil}(x,y)dxdy \tag{5.32}$$

The instantaneous convective heat flux, $q''_{ceil}(x,y)$ can be determined as derived by Cooper [70] as

$$q''_{ceil}(x,y) = h(T_{ad} - T_{ceil}) \tag{5.33}$$

where T_{ad} is a characteristic ceiling jet temperature that would be measured adjacent to an adiabatic lower ceiling surface, and h is a heat transfer coefficient. h and T_{ad} are given by

$$\frac{h}{\tilde{h}} = \begin{cases} 8.82 Re_H^{-1/2} Pr^{-2/3} \left(1 - \left(5 - 0.284 Re_H^{2/5}\right) \frac{r}{H}\right) & 0 \le \frac{r}{H} < 0.2 \\ 0.283 Re_H^{0.3} Pr^{-2/3} \left(\frac{r}{H}\right)^{-1.2} \frac{\frac{r}{H} - 0.0771}{\frac{r}{H} + 0.279} & 0.2 \le \frac{r}{H} \end{cases} \tag{5.34}$$

$$\frac{T_{ad} - T_u}{T_u {Q_H^*}^{2/3}} = \begin{cases} 10.22 - 14.9 \frac{r}{H} & 0 \le \frac{r}{H} < 0.2 \\ 8.39 f\left(\frac{r}{H}\right) & 0.2 \le \frac{r}{H} \end{cases} \tag{5.35}$$

where

$$f\left(\frac{r}{H}\right) = \frac{1 - 1.10\left(\frac{r}{H}\right)^{0.8} + 0.808\left(\frac{r}{H}\right)^{1.6}}{1 - 1.10\left(\frac{r}{H}\right)^{0.8} + 2.20\left(\frac{r}{H}\right)^{1.6} + 0.690\left(\frac{r}{H}\right)^{2.4}} \tag{5.36}$$

$$r = \sqrt{\left(X - X_{fire}\right)^2 + \left(Y - Y_{fire}\right)^2} \tag{5.37}$$

$$\tilde{h} = \rho_u c_p g^{1/2} H^{1/2} {Q_H^*}^{1/3} \ , \ Re_H = \frac{g^{1/2} H^{3/2} {Q_H^*}^{1/3}}{\nu_u} \ , \ Q_H^* = \frac{Q}{\rho_u c_p T_u g^{1/2} H^{5/2}} \tag{5.38}$$

$$Q = \begin{cases} Q_{f,C}\left(\frac{\sigma \dot{M}^*}{1+\sigma}\right) & Z_{fire} < Z_{layer} < Z_{ceil} \\ Q_{f,C} & \begin{matrix} Z_{fire} \ge Z_{layer} \\ Z_{layer} = Z_{ceil} \end{matrix} \end{cases} , \ \dot{M}^* = \begin{cases} 0 & -1 < \sigma \le 0 < 0.2 \\ \frac{1.04599\sigma + 0.360391\sigma^2}{1 + 1.37748\sigma + 0.360391\sigma^2} & \sigma > 0 \end{cases} \tag{5.39}$$

$$\sigma = \frac{1 - \frac{T_u}{T_l} + C_T {Q_{EQ}^*}^{2/3}}{\frac{T_u}{t_l}} \ , \ C_T = 9.115 \ , \ Q_{EQ}^* = \left(\frac{0.21 Q_{fc}}{c_p T_l \dot{m}_p}\right) \tag{5.40}$$

In the above, H is the distance from the (presumed) point source fire and the ceiling, X_{fire} and Y_{fire} are the position of the fire in the room, Pr is the Prandtl number (taken to be 0.7) and ν is the kinematic viscosity of the upper layer gas which is assumed to have the properties of air and can be estimated from $\nu = 0.04128 x 10^7 T_u^{5/2}/(T_u + 110.4)$. Q_H^* and Q_{EQ}^* are dimensionless numbers and are measures of the strength of the plume at the ceiling and the layer interface, respectively.

When the ceiling jet is blocked by the wall surfaces, the rate of heat transfer to the surface increases. Reference [70] provides details of the calculation of wall surface area and convective heat flux for the wall surfaces.

Chapter 6

Fire Protection Devices

6.1 Heat Detectors

Heat detection is modeled using temperatures obtained from the ceiling jet [70]. Rooms without fires do not have ceiling jets. Sensors in these types of rooms use gas layer temperatures instead of ceiling jet temperatures. The characteristic detector temperature is simply the temperature of the ceiling jet (at the location of the detector). The characteristic heat detector temperature is modeled using the differential equation [74]

$$\frac{dT_L}{dt} = \frac{\sqrt{v(t)}}{RTI}(T_g(t) - T_L(t)) \ , \ T_L(0) = T_g(0) \tag{6.1}$$

where T_L and T_g are the link and gas temperatures, v is the gas velocity, and RTI (response time index) is a measure of the sensor's sensitivity to temperature change (thermal inertia). The heat detector differential eq (6.1) may be rewritten to

$$\frac{dT(t)}{dt} = a(t) - b(t)T(t) \ , \ T(t_0) = T_0 \tag{6.2}$$

where $a(t) = \frac{\sqrt{V(t)}T(t)}{RTI}$ and $b(t) = \frac{\sqrt{V(t)}}{RTI}$. Equation (6.2) may be solved using the trapezoidal rule to obtain

$$\frac{T_{i+1} - T_i}{\Delta T} = \frac{1}{2}((a_i - b_i T_i) + (a_{i+1} - b_{i+1} T_{i+1})) \tag{6.3}$$

where the subscript i denotes time at t_i. Equation (6.3) may be simplified to

$$T_{i+1} = A_{i+1} - b_{i+1} T_{i+1} \tag{6.4}$$

where $A_{i+1} = T_i + \frac{\Delta t}{2}(a_i - b_i T_i + a_{i+1})$ and $B_{i+1} = \frac{\Delta t}{2} b_{i+1}$ which has a solution

$$T_{i+1} = \frac{A_{i+1}}{1 + B_{i+1}} = \frac{1 - \frac{\Delta t}{2} b_i}{1 + \frac{\Delta t}{2} b_{i+1}} T_i + \frac{\Delta T}{1 + \frac{\Delta t}{2} b_{i+1}} \left(\frac{a_i + a_{i+1}}{2} \right) \tag{6.5}$$

Equation (6.5) reduces to the trapezoidal rule for integration when $b(t) = 0$. When $a(t)$ and $b(t)$ are constant (the gas temperature, T_g, and gas velocity, V are not changing), eq (6.1) has the solution

$$T(t) = \frac{a}{b} + \frac{e^{-b(t-t_0)}(bT_0 - a)}{b} = T_g + e^{\frac{-\sqrt{V(t)}(t-t_0)}{RTI}}(T_0 - T_g) \tag{6.6}$$

6.2 Sprinkler Activation and Fire Attenuation

For suppression, the sprinkler is modeled using a simple model [75] generalized for varying sprinkler spray densities [76]. It is then modeled by attenuating all fires in the room where the sensor activated by a term of the form $e^{-(t-t_{act})/t_{rate}}$ where t_{act} is the time when the sensor activated and t_{rate} is a constant determining how quickly the fire attenuates. The term t_{rate} can be related to spray density of a sprinkler using a correlation developed in [76]. The suppression correlation was developed by modifying the heat release rate of a fire. For $t > t_{act}$ the heat release is given by

$$Q_f(t) = e^{-(t-t_{act})/\left(3Q_{spray}^{-1.8}\right)} Q_f(t_{act}) \tag{6.7}$$

where Q_{spray} is the spray density of a sprinkler. Note that decay rate can be formulated in terms of either the attenuation rate or the spray density. t_{rate} can be expressed in terms of Q_{spray} as $t_{rate} = 3Q_{spray}^{-1.8}$. A calculation is done to make sure that the fuel burned is consistent with the available oxygen. Once detection has occurred, then the mass and energy release rates are attenuated by

$$\dot{m}_f(t) = e^{-(t-t_{act})/t_{rate}} \dot{m}_f(t_{act}) \tag{6.8}$$

$$Q_f(t) = e^{-(t-t_{act})/t_{rate}} Q_f(t_{act}) \tag{6.9}$$

There are assumptions and limitations in this approach. Its main deficiency is that it assumes that sufficient water is applied to the fire to cause a decrease in the rate of heat release. This suppression model cannot handle the case when the fire overwhelms the sprinkler. The suppression model as implemented does not include the effect of a second sprinkler. Detection of all sprinklers are noted but their activation does not make the fire go out any faster. Further, multiple fires in a room imply multiple ceiling jets. It is not clear how this should be handled, i.e.,how two ceiling jets should interact. When there is more than one fire, the detection algorithm uses the fire that results in the worst conditions (usually the closest fire) in order to calculate the fire sensor temperatures. Finally, the ceiling jet algorithm that we use results in temperature predictions that are warmer (for a given heat release rate) than those used in the correlation developed by Madrzykowski [77], which will cause activation sooner than expected.

6.3 Species Concentration and Deposition

CFAST uses a combustion chemistry scheme based on a carbon-hydrogen-oxygen balance. The scheme is applied in three places. The first is burning in the portion of the plume which is in the lower layer of the compartment of fire origin. The second is the portion in the upper layer, also in the compartment of origin. The third is in the vent flow which entrains air from a lower layer into an upper layer in an adjacent compartment. Included in the combustion calculation is the generation and transport of a number of species that may be produced by a fire. These species include unburned fuel, nitrogen, oxygen, carbon monoxide, carbon dioxide, hydrogen, carbon

(assumed to be soot produced by the fire), hydrogen cyanide, hydrogen chloride, and an arbitrary trace species.

6.3.1 Species Transport

The species transport in CFAST is primarily a matter of bookkeeping to track individual species mass as it is generated by a fire, transported through vents, or mixed between layers in a compartment. When the layers are initialized at the start of the simulation, they are set to ambient conditions. These are the initial temperature prescribed by the user, and 23 % by mass fraction (21 % by volume fraction) oxygen, 77 % by mass fraction (79 % by volume fraction) nitrogen, a mass concentration of water prescribed by the user as a relative humidity, and a zero concentration of all other species. As fuel is burned, the various species are produced in direct relation to the mass of fuel burned (this relation is the species yields prescribed by the user for the fuel burning). Since oxygen is consumed rather than produced by the burning, the 'yield' of oxygen is negative, and is set internally to correspond to the amount of oxygen used to burn the fuel (within the constraint of available oxygen limits discussed in sec. **??**). Two special separate species calculations are included in the model, a time-integrated value for a generic toxic species, Ct, and an arbitrary trace species, TS. Both are assumed not to be part of the overall mass balance, but are rather generated by a fire and transported through a structure in a manner identical to other species.

Each unit mass of a species produced by a fire is carried in the flow to the various rooms and accumulates in the layers. The model keeps track of the mass of each species in each layer, and knows the volume of each layer as a function of time. The mass divided by the volume is the mass concentration, which along with the relative molecular mass gives the concentration in volume percent or parts per million as appropriate. Filters can be used in mechanical ventilation systems to remove species. The phenomenon has been implemented in CFAST to remove trace species and soot. It is implemented by modifying the source terms which describe gas flow. Mass that is filtered remains on the filter and is removed from the air stream. Both the resulting species density and total species removed can be analyzed. See reference [36] for an example on the use of filtering.

The calculation of radiation exchange in CFAST also depends in part on the species concentrations calculated by the model (and thus the user inputs for species yields). There are two separate radiation calculations done by CFAST. The first is for broadband radiation transfer for energy balance. The way this calculation is done is discussed in section 5.0.4. The second is a visible light calculation to answer the question of whether exit signs will be visible. The absorption of broadband radiation depends on the concentration of water, carbon dioxide and soot. The visibility calculation depends solely on the soot concentration For soot, the input for soot yield assumes all the excess carbon goes to soot). This soot generation is then transported as a species to yield a soot mass concentration to use in the optical density calculation based originally on the work of Seader and Einhorn [78]. The most recent work is by Mulholland and Croakin[79]. Based on their experimental measurements, the soot mass density is multiplied by 3,817 m^2/kg (formerly 3,500 m^2/kg) to obtain an optical density (in units of m^{-1}) which is the value reported by the model.

6.3.2 HCl Deposition

Hydrogen chloride produced in a fire can produce a strong irritant reaction that can impair escape from the fire. It has been shown [80] that significant amounts of the substance may be removed by adsorption by surfaces which contact smoke. In our model, HCl production is treated in a manner similar to other species. However, an additional term is required to allow for deposition on, and subsequent absorption into, material surfaces.

The physical configuration that we are modeling is a gas layer adjacent to a surface (Fig. 6.1). The gas layer is at some temperature T_g with a concomitant density of hydrogen chloride, ρ_{HCl}. The mass transport coefficient is calculated based on the Reynolds analogy with mass and heat transfer; that is, hydrogen chloride is mass being moved convectively in the boundary layer, and some of it simply sticks to the wall surface rather than completing the journey during the convective roll-up associated with eddy diffusion in the boundary layer. The boundary layer at the wall is then in equilibrium with the wall. The latter is a statistical process and is determined by evaporation from the wall and stickiness of the wall for HCl molecules. This latter is greatly influenced by the concentration of water in the gas, in the boundary layer and on the wall itself.

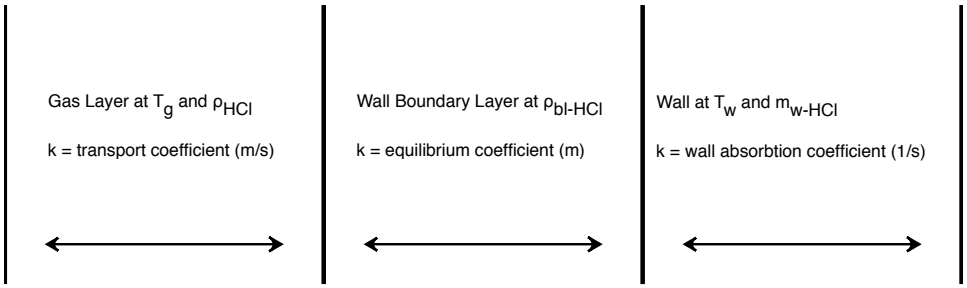

Figure 6.1: Schematic of hydrogen chloride deposition region.

The rate of addition of mass of hydrogen chloride to the gas layer is given by

$$\frac{d}{dt}m_{HCl} = source - k_c(\rho_{HCl} - \rho_{bl-HCl})A_w \tag{6.10}$$

where source is the production rate from the burning object plus flow from other compartments. For the wall concentration, the rate of addition is

$$\frac{d}{dt}d_{w-HCl} = k_c(\rho_{HCl} - \rho_{bl-HCl}) - k_s m_{w-HCl} \tag{6.11}$$

where the concentration in the boundary layer, ρ_{bl-HCl} is related to the wall surface concentration by the equilibrium constant k_e, by the relation $\rho_{bl-HCl} = d_{w-HCl}/k_e$. We never actually solve for the concentration in the boundary layer, but it is available, as is a boundary layer temperature if it were of interest. The transfer coefficients are

$$k_c = \frac{\dot{q}}{\Delta T \rho_g c_p} \tag{6.12}$$

$$k_e = \frac{b_1 e^{1500/T_w}}{1 + b_2 e^{1500/T_w}\rho_{HCl}}\left(1 + \frac{b_5(\rho_{H_2O})^{b_6}}{\left(\rho_{H_2O,sat} - \rho_{H_2O,g}\right)^{b_7}}\right) \tag{6.13}$$

Table 6.1: Transfer coefficients for HCl deposition

Surface	b_1 (m)	b_2 (m^3/kg)	b_3 (s^{-1})	b_4 (J/g mol)	b_5 (m^3/kg)$^{b_7-b_6}$	b_6 (note a)	b_7 (note b)
Painted Gypsum	0.0063	191.8	0.0587	7476	193	1.021	0.431
PMMA	$9.6x10^{-5}$	0.0137	0.0205	7476	29	1.0	0.431
Ceiling Tile	$4.0x10^{-3}$	0.0548	0.123	7476	30[a]	1.0	0.431
Cement Block	$1.8x10^{-2}$	5.48	0.497	7476	30[a]	1.0	0.431
Calcium Silicate Board	$1.9x10^{-2}$	0.137	0.030	7476	30[a]	1.0	0.431

a - very approximate value, insufficient data for high confidence value
b - non-dimensional

$$k_s = b_3 e^{-\left(\frac{b_4}{RT_w}\right)} \tag{6.14}$$

The only values currently available for these quantities are shown in table 6.1 [81]. The "b" coefficients are parameters which are found by fitting experimental data to the above equations. These coefficients reproduce the adsorption and absorption of HCl reasonably well. Note though that error bars for these coefficients have not been reported in the literature.

The experimental basis for poly(methyl methacrylate) and gypsum cover a sufficiently wide range of conditions that they should be usable in a variety of practical situations. The parameters for the other surfaces do not have much experimental backing, and so their use should be limited to comparison purposes.

6.4 Single Zone Approximation

A single zone approximation is appropriate for smoke flow far from a fire source where the two-zone layer stratification is less pronounced than in compartments near the fire. In this situation, a single zone approximation may be derived by using the normal two-zone source terms and the substitutions:

$$\begin{aligned} \dot{m}_U^{new} &= \dot{m}_L + \dot{m}_U \\ \dot{m}_L^{new} &= 0 \\ Q_U^{new} &= Q_L + Q_U \\ Q_L^{new} &= 0 \end{aligned} \tag{6.15}$$

This is used in situations where the stratification does not occur. Examples are elevators shafts, complex stairwells, natural venting ductwork, and compartments far from the fire.

Chapter 7

Mathematical and Numerical Robustness

The mathematical and numerical robustness of a deterministic computer model depends upon three issues: the code must be transparent so that it can be understood and modified by visual inspection; it must be possible to check and verify with automated tools; and there must be a method for checking the correctness of the solution, at least for asymptotic (steady state) solutions (numerical stability and agreement with known solutions).

In order to understand the meaning of accuracy and robustness, it is necessary to understand the means by which the numerical routines are structured. In this chapter, details of the implementation of the model are presented, including the tests used to assess the numerical aspects of the model. These include

- the structure of the model, including the major routines implementing the various physical phenomena included in the model,
- the organization of data initialization and data input used by the model,
- the structure of data used to formulate the differential equations solved by the model,
- a summary of the main control routines in the model that are used to control all input and output, initialize the model and solve the appropriate differential equation set for the problem to be solved,
- the means by which the computer code is checked for consistency and correctness,
- analysis of the numerical implementation for stability and error propagation, and
- comparison of the results of the system model with simple analytical or numerical solutions.

7.1 Structure of the Numerical Routines

A methodology which is critical to verification of the model is the schema used to incorporate physical phenomena. This is the subroutine structure discussed below. The method for incorporating new phenomena and insuring the correctness of the code was adopted as part of the consolidation of CCFM and FAST. This consolidation occurred in 1990 and has resulted in a more transparent,

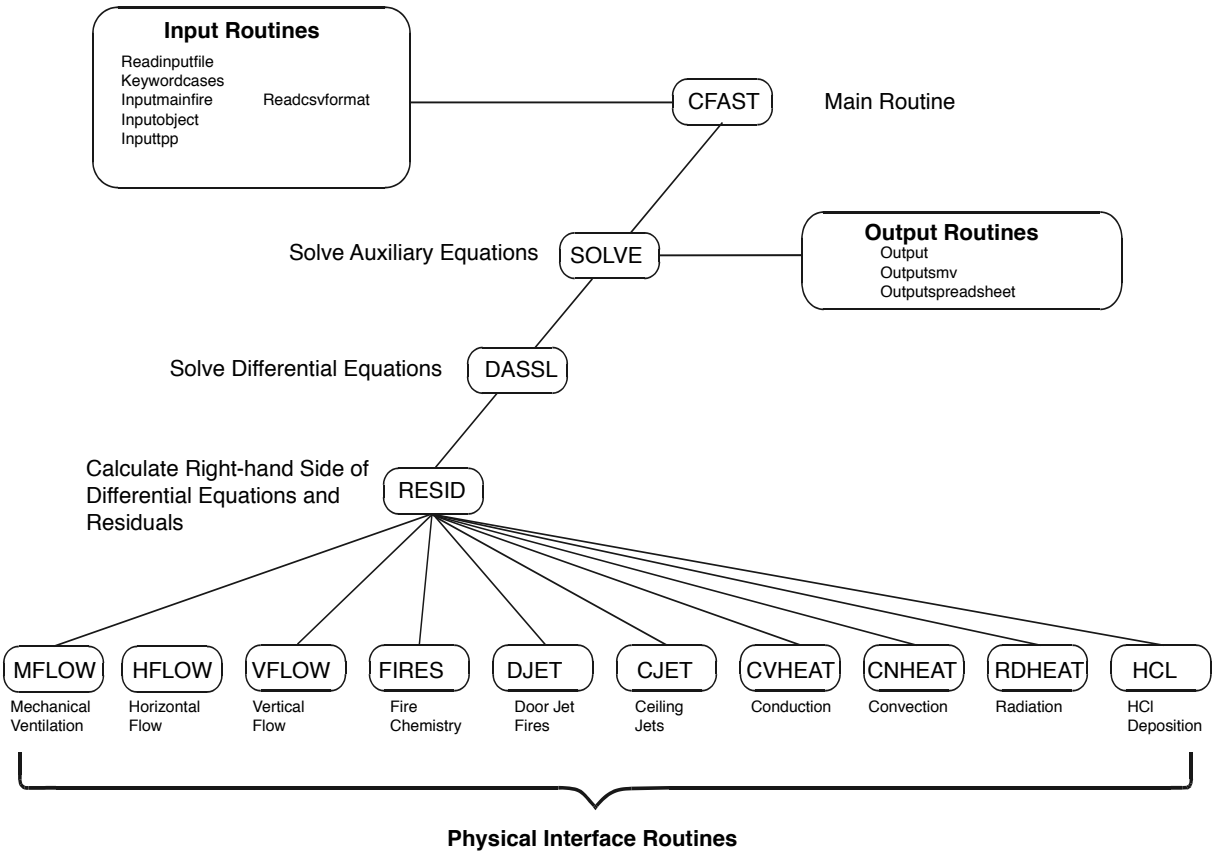

Figure 7.1: Subroutine structure for the CFAST model.

transportable and verifiable numerical model. This transparency is crucial to a verifiable and robust numerical implementation of the predictive model as discussed in the sections on code checking and numerical analysis.

The model can be split into distinct parts. There are routines for reading data, calculating results and reporting the results to a file or printer. The major routines for performing these functions are identified in figure 7.1. These physical interface routines link the CFAST model to the actual routines which calculate quantities such as mass or energy flow at one particular point in time for a given environment.

The routines SOLVE, RESID and DASSL are the key to understanding how the physical equations are solved. SOLVE is the control program that oversees the general solution of the problem. It invokes the differential equation solver DASSL [82] which in turn calls RESID to solve the transport equations. Given a solution at time t, what is the solution at time t plus a small increment of time, Δt, (where the time increment is determined dynamically by the program to insure convergence of the solution at $t + \Delta t$)? The differential equations are of the form

$$\frac{dy}{dt} = f(y,t) \ , \ y(t_0) = y_0 \tag{7.1}$$

where y is a vector representing pressure, layer height, mass and such, and f is a vector function that represents changes in these values with respect to time. The term y_0 is an initial condition at

the initial time t_0 . The subroutine RESID computes the right hand side of eq (7.1) and returns a set of residuals of that calculation to be compared to the values expected by DASSL. DASSL then checks for convergence. Once DASSL reaches an error limit (defined as convergence of the equations) for the solution at $t + \Delta t$, SOLVE then advances the solution of species concentra- tion, wall temperature profiles, and mechanical ventilation for the same time interval. Note that there are several distinct time scales that are involved in the solution of this type of problem. The fastest will be chemical kinetics. We avoid that scale by assuming that the chemistry is infinitely fast. The next larger time scale is that associated with the flow field. These are the equations which are cast into the form of ordinary differential equations. Then there is the time scale for mechanical ventilation, and finally, heat conduction through objects. Chemical kinetic times are typically on the order of milliseconds. The transport time scale are on the order of 0.1 s. The mechanical ventilation and conduction time scales are typically several seconds, or even longer. The time step is dynamically adjusted to a value appropriate for the solution of the currently defined equation set. In addition to allowing a more correct solution to the pressure equation, very large time steps are possible if the problem being solved approaches steady-state.

7.2 Code Checking

There are two means to automate checking the correctness of the language used by a numerical model. The first is the use of standard methods for checking the structure and interface. Programs such as Flint and Lint are standard tools to do such checking. They are applied to the whole model. There are three aspects of the model checked by this procedure: correctness of the interface, undefined or incorrectly defined (or used) variables and constants, and completeness of loops and threads. It does not check for the correctness of the numerical use of constants or variables only that they are used correctly in a syntactical sense. Lint is part of most C language distributions of Unix. Flint is the equivalent for the FORTRAN language. Though it is not usually included with FORTRAN distributions Flint is generally available [1]. Both have been used with CFAST.

The second is to use a variety of computer platforms to compile and run the code. Since FORTRAN and C are implemented differently for various computers, this represents both a numerical check as well as a syntactic check. CFAST has been compiled for the Sun (Solaris), SGI (Irix), the windows-based PCs (Lahey, Digital, and Intel FORTRAN), and the Concurrent Computer platforms. Within the precision afforded by the various hardware implementations, the answers are identical [2].

7.3 Numerical Tests

There are two components to testing the numerical solutions of CFAST. First, the DASSL solver is well tested for a wide variety of differential equations, and is widely used and accepted [82]. Also, the radiation and conduction routines are tested with known solutions. These are not analytical tests, but physical limits, such as an object immersed in a fluid of constant temperature, to

[1] Cleanscape Software, 445 Sherman Ave, Ste. Q, Palo Alto, CA 94306

[2] Typically one part in 10^{-6}, which is the error limit used for DASSL.

which the temperature must equilibrate. The solver(s) must show that the differential equations asymptotically converge to these answers.

The second is to insure that the coupling between algorithms and the solver is correct. Most errors are avoided because of the structure discussed in section 7.1. The error due to the numerical solution is far less than that associated with the model assumptions. Two examples of this are the coupling of mechanical ventilation with buoyant flow, and the Nusselt number assumption for boundary layer convection. For the former, the coupling of a network of incompressible flow with an ODE for compressible flow has to deal with disparate calculations of pressure. For the latter, a very small time step occurs when a floor is heated and the thermal wave reaches the far (unexposed) side. This is a limitation of the physical implementation of the heat flow algorithm (convection). The solver arrives at the correct solution, but the time step becomes very small in order to achieve this.

Numerical error can be divided into three categories: roundoff, truncation and discretization error. Roundoff error occurs because computers represent real numbers using a finite number of digits. Truncation error occurs when an infinite process is replaced by a finite one. This can happen, for example, when an in finite series is truncated after a finite number of terms or when an iteration is terminated after a convergence criterion has been satisfied. Discretization error occurs when a continuous process such as a derivative is approximated by a discrete analog such as a divided difference. CFAST is designed to use 64-bit precision for real number calculations to minimize these effects.

Implicit in solving the equations discussed in chapter 2, is that the solver will arrive at a solution. Inherent in the DASSL solver are convergence criteria for the mass and energy balance within CFAST to insure mass and energy conservation within 1 part in 10^6. There are, however, limitations introduced by the algorithmic realization of physical models, that can produce errors and instabilities. Using the example above, if a mechanical ventilation system injects or removes mass and enthalpy from a small duct, then there can be a stability issue with the layer interface bobbing up and down over the duct. These are annoyances to the user community and shortcomings of the implementation of algorithm rather than failure of the system model.

Problems of this sort are noted in the frequently asked questions on the CFAST web site (http://cfast.nist.gov).

7.4 Comparison with Analytic Solutions

There do not exist general analytic solutions for fire problems, even for the simplest cases. That is, there are no closed form solutions to this type of problem. However, it is possible to do two kinds of checking. The first type is discussed in the section on the theoretical basis of the model, for which individual algorithms are validated against experimental work. The second is simple experiments, especially for conduction and radiation, for which the results are asymptotic. For example, for a simple, single compartment test case with no fire, all temperatures should equilibrate asymptotically to a single value. Such comparisons are common and not usually published.

Chapter 8

Sensitivity of the Model

A sensitivity analysis considers the extent to which uncertainty in model inputs influences model output. For a sensitivity analysis, this uncertainty includes not only that inherent in the input of data for specific scenarios by the model user, but also uncertainty in empirical data or numerical parameters in the model such as the time step size used by the model to obtain a solution.

Among the purposes for conducting a sensitivity analysis are to determine

- the important variables in the models,
- the computationally valid range of values for each input variable, and
- the sensitivity of output variables to variations in input data.

Conducting a sensitivity analysis of a complex model is not a simple task and it will differ depending on the application. CFAST typically requires the user to provide numerous input parameters that describe the building geometry, compartment connections, construction materials, and description of one or more fires.

Iman and Helton [83] studied the sensitivity of complex computer models developed to simulate the risk of severe nuclear accidents which may include fire and other risks. Consistent with the work of Iman and Helton [83], ASTM E1355 [1] provides overall guidance on typical areas of evaluation of the sensitivity of deterministic fire models. These areas may involve one or more of the following techniques: finite difference or direct analysis methods that provide an explicit solution of the sensitivity equations associated with the governing equations of the model, factorial design or Latin hypercube sampling studies that investigate the effect of varying the input parameters and consequential interactions between parameters that may be deemed important, and global or response surface methods that investigate the overall behavior of model outputs for a desired range of inputs.

This chapter provides a review of the sensitivity studies that have been conducted using CFAST with an emphasis on uncertainty in the input. Other sensitivity investigations of CFAST are also available [84, 85, 86].

8.1 Factorial Design Studies

Khoudja [[87] has studied the sensitivity of an early version of the FAST [2] (predecessor to CFAST) model with a fractional factorial design involving two levels of 16 different input pa-

rameters. The statistical design, taken from the texts by Box and Hunter [88], and Daniel [89] reduced the necessary model runs from more than 65 000 to 256 by studying the interactions of input parameters simultaneously. The choice of values for each input parameter represented a range for each parameter. The analysis of the FAST model showed sensitivity to heat loss to the compartment walls and to the number of compartments in the simulation. Without the inclusion of surface thermophysical properties, this model treats surfaces as adiabatic for conductive heat transfer. Thus, consistent sensitivity should be expected. Sensitivity to changes in thermal properties of the surfaces were not explored.

Walker [90] discussed the uncertainties in components of zone models and showed how uncertainty within user-supplied data affects the results of calculations using CFAST as an example. The study systematically varied inputs related to the fire (heat release rate, heat of combustion, mass loss rate, radiative fraction, and species yields) and compartment geometry (vent size and ceiling height) ranging from $\pm$ 1 % to $\pm$ 20 % of base values for a one- compartment scenario. Heat release rate and ceiling height are seen to be the dominant input variables in the simulations. Upper layer temperature changed $\pm$ 10 % for a $\pm$ 10 % change in heat release rate. Typical variation of $\pm$ 10 s in time to untenable conditions for a 20 % variation in the inputs was noted for the scenarios studied.

Peacock et al. [84] studied the sensitivity of CFAST for a range of input parameters. They used simple factorial designs for model inputs deemed important to investigate local behavior of important model outputs along with response surface methods to evaluate overall model behavior. Results of the parametric investigations are discussed below and the application of response surface methods is summarized in section 5.2. Both are discussed in more detail in reference [84].

8.1.1 Model Inputs and Outputs

Most studies of modeling related to fire hazard and fire reconstruction present a consistent set of variables of interest to the model user [91, 92, 85, 93] : upper and lower gas layer temperatures, gas species concentrations, and layer interface position. Other variables of interest include

- mass pyrolysis and heat release rate,
- room pressure, and
- vent flow.

Although there are certainly other comparisons of interest, these will provide evidence of the sensitivity of the model to most model inputs. Tables 4 and 5 show typical inputs and outputs for the CFAST model.

Consider the following fire scenario: The building geometry (figure 8.1) includes four rooms on two floors with horizontal, vertical, and mechanical vents connecting the rooms and venting to the outdoors. The fire source in one of the rooms on the lower floor is a medium growth rate t-squared fire [94] chosen to simulate a mattress fire [95].

Sensitivity to Small Changes in Model Inputs

To investigate the sensitivity of the model, a number of simulations were conducted varying the input parameters about the base scenario discussed in the previous section. Both small ($\pm$10 %) and

Table 8.1: Typical Inputs for a Two-Zone Fire Model

Ambient Conditions	Inside temperature and pressure. Outside temperature and pressure. Wind speed. Relative humidity
Building Geometry	Compartment width, depth, height, and surface material properties (conductivity, heat capacity, density, thickness). Horizontal Flow Vents: Height of soffit above floor, height of sill above floor, width of vent, angle of wind to vent, time history of vent openings and closings. Vertical Flow Vents: Area of vent, shape of vent. Mechanical Ventilation, Orientation of vent, Center height of vent, area of vent, length of ducts, diameter of ducts, duct roughness, duct flow coefficients, fan flow characteristics.
Fire Specification	Fire room, X, Y, Z position in room, fire area. Fire Chemistry: Molar Weight, Lower oxygen limit, heat of combustion, initial fuel temperature, gaseous ignition temperature, radiative fraction. Fire History: Mass loss rate, heat release rate, species yields for HCN, HCl, H/C, O_2/C, C/CO_2, CO/CO_2.

Table 8.2: Typical Outputs for a Two-Zone Fire Model

Environment	for each compartment: Compartment pressure and layer interface height. for each layer and compartment: Temperature, layer mass density, layer volume, heat release rate, gas concentrations (N2, O2, CO2, CO, H2O, HCl, HCN, soot optical density), radiative heat into layer, convective heat into layer, heat release rate in layer. for each vent and layer: Mass flow, entrainment, vent jet fire. for each fire: Heat release rate of fire, mass flow from plume to upper layer, plume entrainment, pyrolysis rate of fire. for each compartment surface: Surface temperatures.
Tenability	Temperature. Fractional Effective Dose (FED).

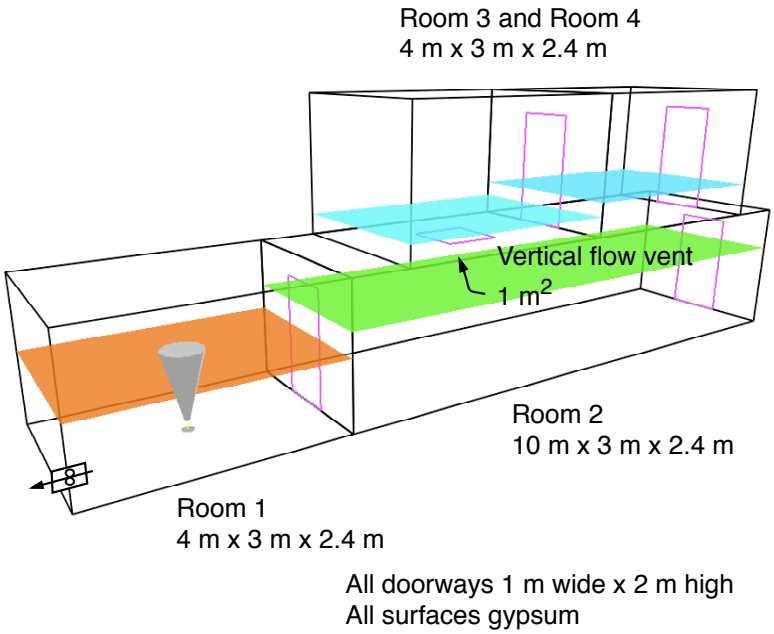

Figure 8.1: Building Geometry for base case scenario.

larger (up to an order of magnitude) variations for selected inputs were studied. Varying most of the inputs by small amounts had little effect on the model outputs. Figure 8.2 presents an example of the time dependent sensitivity of several outputs to a 10 % change in room volume for the fire compartment in the scenario described above. For example, the pair of dotted-line curves labeled Upper Layer Volume were created by comparing the base case scenario with a scenario whose compartment volume was increased and decreased by 10 %. The resulting curves presented on the graph are the relative difference between the variant cases and the base case defined by (Variant value - Base value) / Base value for each time point. The graph shows that temperature and pressure are insensitive to changes in the volume of the fire room since a 10 % change in room volume led to smaller relative changes in layer temperature and room pressure for all times. Upper layer volume can be considered neutrally sensitive (a 10 % change in room volume led to about a 10 % change in layer volume). Further, this implies that there is negligible effect on the average layer interface height. This is consistent with both experimental observations in open compartment room fires and analytical solutions for single compartment steady-state fires . For transient conditions early in the fire or when the fire burns out (illustrated in the figure at 300 s when the gas burner fire heat release rate goes to zero) higher uncertainties are noted. While these are transient effects, the early phases of the fire, in particular, may be important in calculating tenability for occupants during egress. While an uncertainty in the compartment volumes results in an equivalent uncertainty in calculated outputs, accurate specification of compartment dimensions within 5 % is often easily obtained.

In addition, figure 8.2 shows a somewhat constant relative difference for the changes as a function of time. As suggested by Iman and Helton [[83], an average relative difference could thus be used to characterize the model sensitivity for comparing individual inputs and outputs.

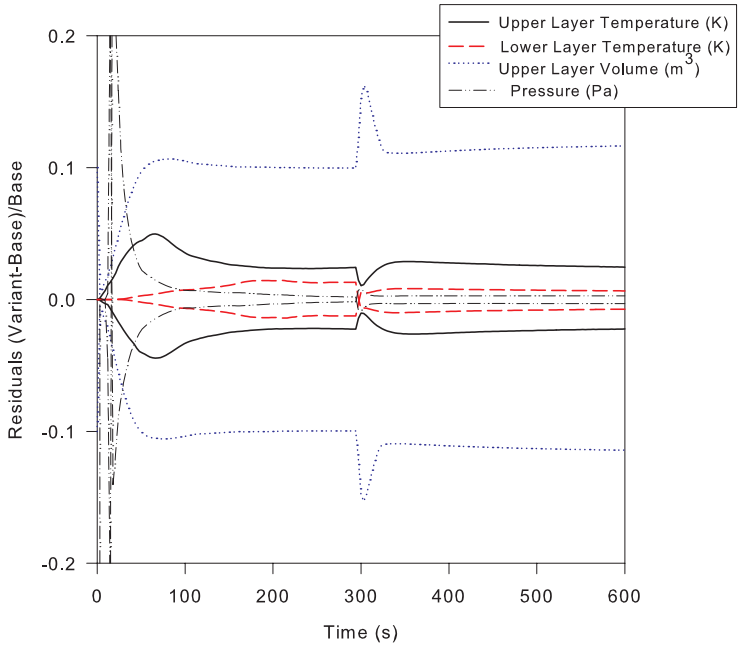

Figure 8.2: An example of time dependent sensitivity of fire model outputs to a 10 % change in room volume for a single room fire scenario.

8.1.2 Sensitivity to Larger Changes in Model Inputs

To investigate the effects of much larger changes in the inputs, a series of simulations was conducted where the inputs were varied from 10 % to 400 % of base values. Simulations changing the heat release rate inputs from the base peak heat release rate of 750 kW are shown in figure 8.3.

Each set appears as families of curves with similar functional forms. This indicates that the heat release rate has a monotonic effect on the layer temperatures, with not as clear an effect on upper layer volume due to compartment filling and flow between compartments. Like the sensitivity to compartment volume in the previous section, changing the heat release rate by a factor of two results in a factor of two change in the upper layer temperature. Thus, in absolute terms, heat release rate and compartment volume are equally sensitive. However, compartment volume is easily determined accurately while heat release rate is typically estimated with far less accuracy and may be uncertain to within an order of magnitude or larger.

In the majority of fire cases, the most crucial question that can be asked by the person responsible for fire protection is: How big is the fire? Put in quantitative terms, this translates to: What is the heat release rate of this fire? Recently the National Institute of Standards and Technology (NIST) examined the pivotal nature of heat release rate measurements in detail [96]. Not only is heat release rate seen as the key indicator of real-scale fire performance of a material or construction, heat release rate is, in fact, the single most important variable in characterizing the flammability of products and their consequent fire hazard. Much of the remainder of this paper focuses on heat release rate as an example for examining sensitivity analysis.

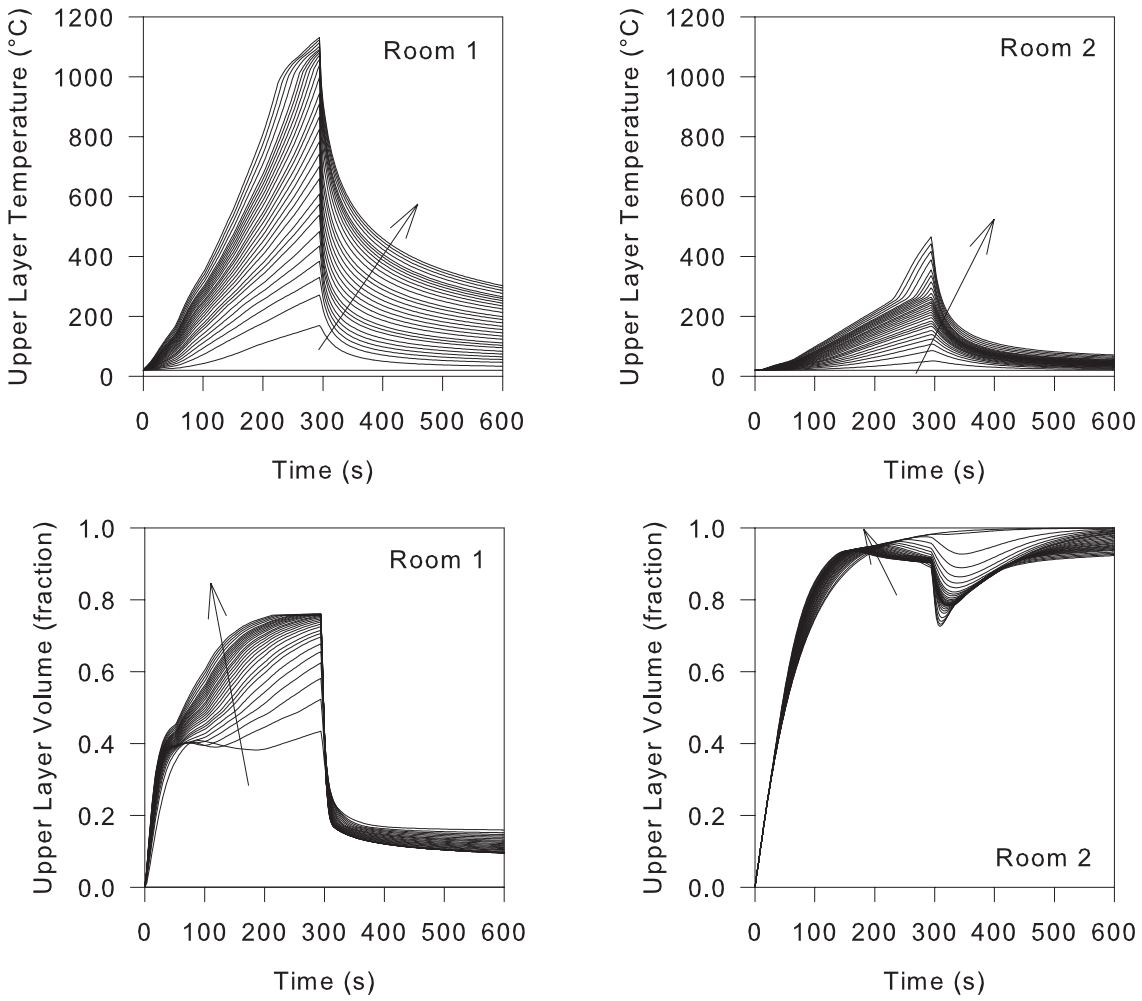

Figure 8.3: Layer temperatures and volumes in several rooms resulting from variation in heat release rate for a four-room growing fire scenario.

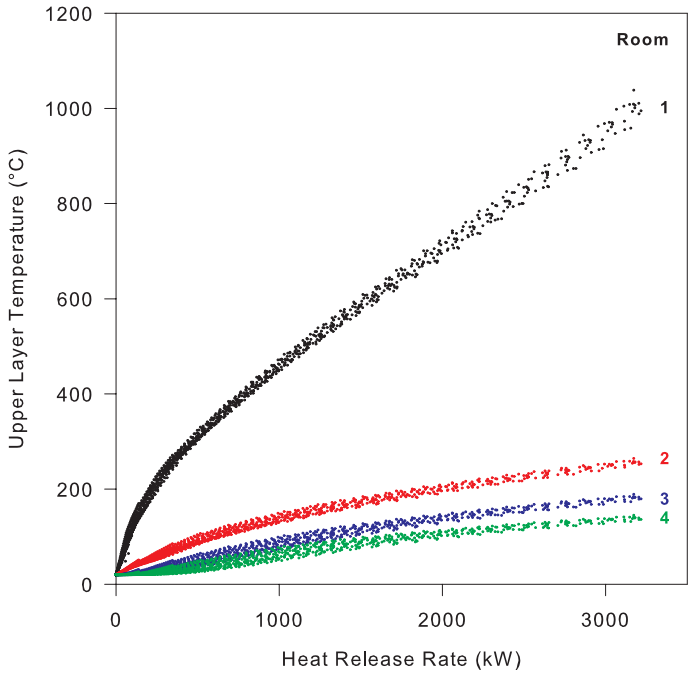

Figure 8.4: Comparison of the time dependent heat release rate and layer temperatures in several rooms for a four-room growing fire scenario.

8.2 Response Surface Studies

A next step beyond the simple plots presented in figure 8.3 is a cross-plot of outputs of interest against heat release rate. Figure 8.4 presents plots of the upper layer temperature (presented in figure 8.3) plotted against the heat release rate for all the simulations. The temperature curves for upper layer temperature in all four rooms (figure 8.4) show a strong functional dependence on heat release rate. Even for the wide variation in inputs, the heat release rate provides a simple predictor of the temperature in the rooms. In addition, this relationship allows calculation of the sensitivity of the temperature outputs to the heat release rate inputs as a simple slope of the resulting correlation between heat release rate and temperature.

Figure 8.5, simply a plot of the slope of the regression curves in figure 8.4, shows this sensitivity, $\partial(T)/\partial(heatreleaserate)$, for the four-room scenarios studied and represents all time points in all he simulations in which the peak heat release rate was varied from 0.1 to 4.0 times the base value. Except for relatively low heat release rate, the upper layer temperature sensitivity is less than 1 K/kW and usually below 0.2 K/kW. Not surprisingly, the layer that the fire feeds directly is most sensitive to changes. The lower layer in the fire room and all layers in other rooms have sensitivities less than 0.2 K/kW. This implies, for example, that if the heat release rate for a 1 MW fire is known to within 100 kW, the resulting uncertainty in the calculation of upper layer temperature in the fire room is about $\pm$ 30 K.

For upper layer volumes (figure 8.6) of both rooms 1 and 2, it is again a simple correlation between heat release rate and volume fraction (upper layer volume expressed as a fraction of the

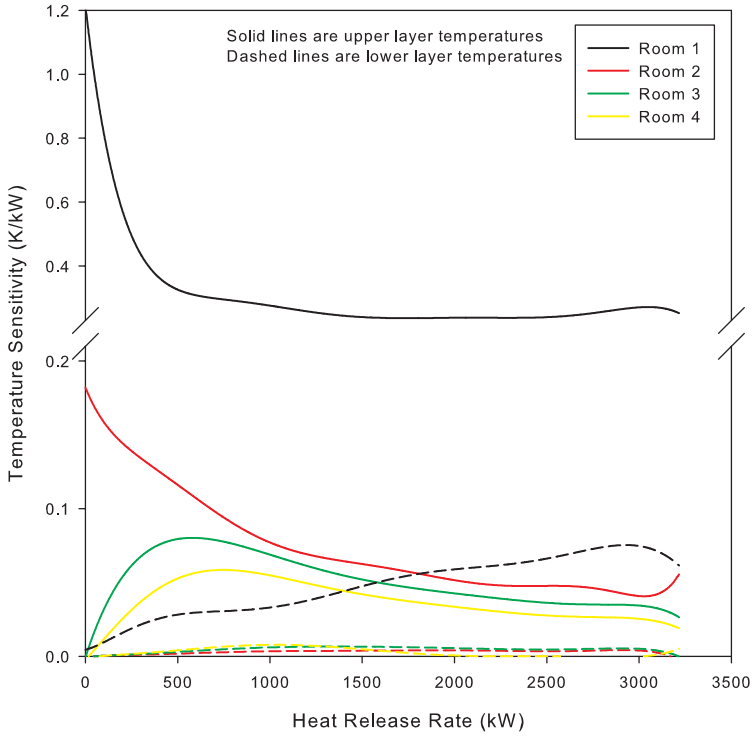

Figure 8.5: Sensitivity of temperature to heat release rate for a four-room growing fire scenario.

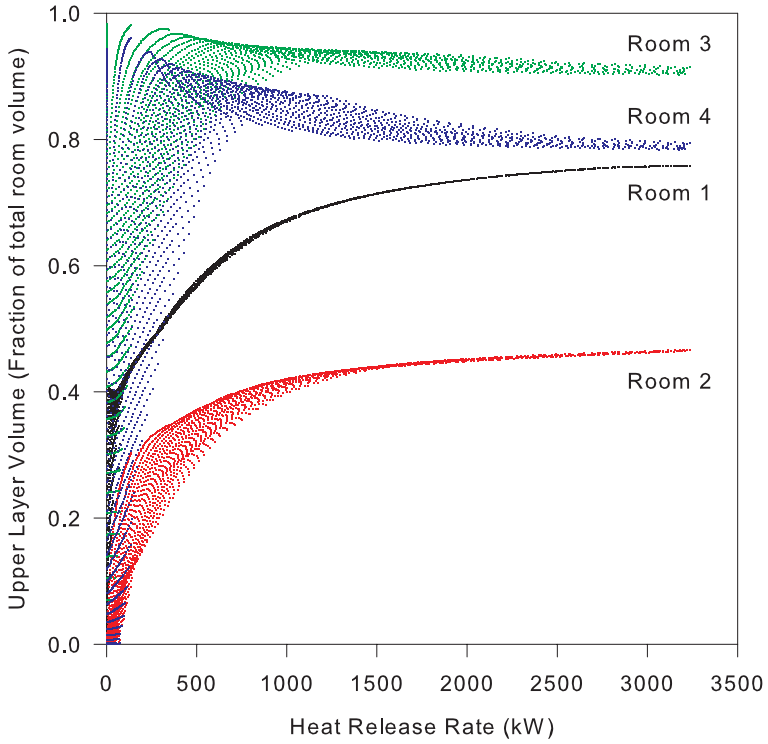

Figure 8.6: Sensitivity of temperature to heat release rate for a four-room growing fire scenario.

total room volume). The shaded gray area on the graph shows the locus of all individual time point values of temperature and volume in the four compartments of the simulation. The correlations for the upper layer volumes of room 1 and room 2 could also be differentiated as was done for the temperature correlations to obtain sensitivities for the upper layer volume. For rooms 3 and 4, the relationship is not as clear. The flow into the layers of these rooms is more complicated than for rooms 1 and 2, resulting from flow from the first floor through a vent in the floor of room 3 and from a vent to the outside in room 4. However, even these rooms approach a constant value for higher heat release rate values, implying near zero sensitivity for high heat release rate.

Figure 8.7 presents the effect of both peak heat release rate and vent opening (in the fire room) on the peak upper layer temperature. In this figure, actual model calculations, normalized to the base scenario values are indicated by circles overlaid on a surface grid generated by a spline interpolation between the data points. At high heat release rate and small vent openings, the fire becomes oxygen limited and the temperature trails off accordingly, but for the most part, the behavior of the model is monotonic in nature. Although more laborious, the approaches used to calculate sensitivities for single variable dependencies illustrated earlier are thus equally applicable to multivariate analyses.

From the surface, it is clear that heat release rate has more of an effect on the peak temperature than does the vent width. Until the fire becomes oxygen limited, the trends evident in the surface are consistent with expectations temperature goes up with rising heat release rate and down with rising vent width. The effects are not, of course, linear with either heat release rate or vent opening.

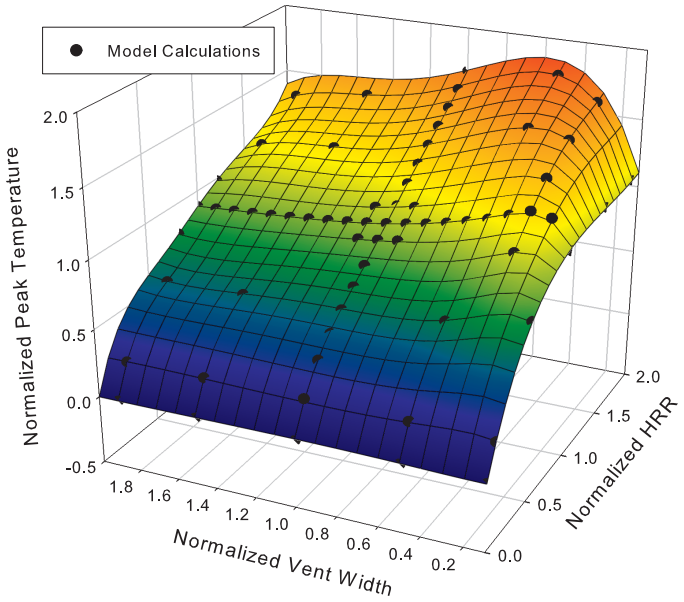

Figure 8.7: Sensitivity of temperature to heat release rate for a four-room growing fire scenario.

Plume theory and typically used algorithms for estimating upper layer temperature in a single room with a fire suggest that the dependence is on the order of $Q_f^{2/3}$ for heat release rate and $A\sqrt{h}$ for the vent opening where A is the area of the vent and h is the height of the vent. Although these correlations are based on a simple analysis of a single room fire, the dependence suggested is similar to that illustrated in figure 8.7.

8.3 Latin Hypercube Sampling Studies

Notarianni [86] developed an iterative methodology for the treatment of uncertainty in fire-safety engineering calculations to identify important model parameters for detailed study of uncertainty. She defines a nine-step process to identify crucial model inputs and parameters, select sampling methods appropriate for the important parameters, and evaluate the sensitivity of the model to chosen outcomes. Both factorial designs and Latin hypercube sampling are included in a case study involving the CFAST model. In a performance-based design of a 16 story residential structure, the impact of model uncertainty on a chosen design and inclusion of residential sprinklers in the design would effect the resulting safety of the design. For a seven-compartment scenario representing one living unit in the structure, distributions of input variables based on Latin hypercube sampling of selected ranges of the inputs were developed and used as input for a series of 500 CFAST simulations for the scenario. The results of the calculations are presented in a series of cumulative distribution functions which show the probability that a chosen criterion of the design is exceeded within a given time. Depending on the evaluation criterion chosen, times to unaccept-

able designs varied by as little as 10 s to as much as 470 s. To determine important input variables, Notarianni used a multivariate correlation of the input and output variables to determine statistical significance at a 95 % confidence level. Input variables deemed important in the analysis included fire-related inputs (growth rate, heat of combustion, position of the base of the fire, and generation rates of products of combustion) and door opening sizes. Other inputs were determined to be less important.

8.4 Summary

Many of the outputs of the CFAST model are quite insensitive to uncertainty in the input parameters for a broad range of scenarios. Not surprisingly, heat release rate was consistently seen as the most important variable in a range of simulations. Heat release rate and related variables such as heat of combustion or generation rates of products of combustion provide the driving force for fire-driven flows. For CFAST, all of these are user inputs. Thus, careful selection of these fire related variables are necessary for accurate predictions. Other variables related to compartment geometry such as compartment height or vent sizes, while deemed important for the model outputs, are typically more easily defined for specific design scenarios than fire related inputs. For some scenarios, such as typical building performance design, these vents may need to include the effects of leakage to insure accurate predictions. For other scenarios, such as shipboard use or nuclear power facilities, leakage (or lack thereof) may be easily defined and may not be an issue in the calculations.

Chapter 9

Summary of Model Validation

CFAST has been subjected to extensive validation studies by NIST and others. There are two ways of comparing predictive capability with actual events. The first is simply graphing the time series curves of model results with measured values of variables such as temperature. Another approach is to consider the time to critical conditions such as flashover. Making such direct comparisons between theory and experiment provides a sense of whether predictions are reasonable. This chapter provides a review of CFAST validation efforts by NIST and others to better understand the quality of the predictions by the model.

Some of the work has been performed at NIST, some by its grantees and some by engineering firms using the model. Because each organization has its own reasons for validating the model, the referenced papers and reports do not follow any particular guidelines. Some of the works only provide a qualitative assessment of the model, concluding that the model agreement with a particular experiment is "good" or "reasonable." Sometimes, the conclusion is that the model works well in certain cases, not as well in others. These studies are included in the survey because the references are useful to other model users who may have a similar application and are interested in qualitative assessment. It is important to note that some of the papers point out flaws in early releases of CFAST that have been corrected or improved in more recent releases. Some of the issues raised, however, are still subjects of active research. Continued updates for CFAST are greatly influenced by the feedback provided by users, often through publication of validation efforts.

A true validation of a model would involve proper statistical treatment of all the inputs and outputs of the model with appropriate experimental data to allow comparisons over the full range of the model. Thus, the comparisons of the differences between model predictions and experimental data discussed here are intentionally simple and vary from test to test and from variable to variable due to the changing nature of the tests and typical use of different variables. Table 9 summarizes the Validation comparisons included for the current version of the model detailed in the Software Development and Experimental Evaluation Guide for CFAST [8].

Four of the quantities were seen to require additional care when using the model to evaluate the given quantity. This typically indicates limitations in the use of the model. A few notes on the comparisons are appropriate:

- CFAST typically predicts plume temperature near to experimental uncertainty, but tends to under-predict temperatures nearer to the fire source and over-predict temperatures farther

away.

- CFAST typically over-predicts smoke concentration. Predicted concentrations for open-door tests are within experimental uncertainties, but those for closed-door tests are far higher.

- With exceptions, CFAST predicts cable surface temperatures within experimental uncertainties. Total heat flux to targets is typically predicted to within about 30 %, and often under-predicted. Radiative heat flux to targets is typically over-predicted compared to experimental measurements, with higher relative difference values for closed-door tests. Care should be taken in predicting localized conditions (such as target temperature and heat flux) because of inherent limitations in all zone fire models.

- Predictions of compartment surface temperature and heat flux are typically within 10 % to 30 %. Generally, CFAST over-predicts the far-field fluxes and temperatures and under-predicts the near-field measurements. This is consistent with the single representative layer temperature assumed by zone fire models.

CFAST predictions in this validation study were consistent with numerous earlier studies, which show that the use of the model is appropriate in a range of fire scenarios. The CFAST model has been subjected to extensive evaluation studies by NIST and others. Although differences between the model and the experiments were evident in these studies, most differences can be explained by limitations of the model as well as of the experiments. Like all predictive models, the best predictions come with a clear understanding of the limitations of the model and the inputs provided to perform the calculations.

Chapter 10

Conclusion

CFAST is a collection of data, computer programs, and documentation which are used to simulate the important time-dependent phenomena describing the character of a compartment fire. The major functions provided include calculation of the buoyancy-driven as well as forced transport of energy and mass through a series of specified compartments and connections (e.g., doors, windows, cracks, ducts), and the resulting temperatures, smoke optical densities, and gas concentrations after accounting for heat transfer to surfaces and dilution by mixing with clean air.

CFAST is a zone model. The basic assumption of all zone fire models is that each compartment can be divided into a small number of control volumes, each of which is internally uniform in temperature and composition. Beyond these basic assumptions, the model typically involves a mixture of established theory (e.g., conservation equations), empirical correlations where there are data but no theory (e.g., flow and entrainment coefficients), and approximations where there are neither (e.g., post-flashover combustion chemistry) or where their effect is considered secondary compared to the cost of inclusion (e.g., temperature dependent material properties)..

The predictive equations are based on the fundamental laws of conservation of mass and energy. Empirical correlations are employed to bridge gaps in existing knowledge. Since the necessary approximations required by operational practicality result in the introduction of uncertainties in the results, the user should understand the inherent assumptions and limitations of the programs, and use these programs judiciously - including sensitivity analyses for the ranges of values for key parameters in order to make estimates of these uncertainties.

As discussed in this report, the CFAST model has been subjected to extensive evaluation studies by NIST and others. Although differences between the model and the experiments were evident in these studies, most differences can be explained by limitations of the model as well as of the experiments. Like all predictive models, the best predictions come with a clear understanding of the limitations of the model and of the inputs provided to do the calculations.

CFAST has proven to be fast, robust and reliable. While the focus of the development of the model has been whole building simulations for assessing the effect of fire on a building environment, principally to calculate threats to life safety of occupants and insults to the building structure, it has been used for a wide variety of building and fire scenarios. The simplest use has been to ascertain the sufficiency of an air handling system to extract smoke. The most complex has been an assessment of fire propagation in a high-rise complex. It is also widely used as the fire model in egress calculations and is described as the basis for hazard estimates in the Simulex [97] and Exodus [98] egress models.

Because of the speed of the model, it is possible to do real parameter studies of the building environment. It is reasonable to do actual parameter studies including the tens of thousands of variations needed for a proper hazard and risk calculation. Even in those cases where more detailed predictions are needed (e.g., smoke detector and sprinkler head siting), CFAST provides the capability to scope the problem, in essence doing parameter studies to determine what specific scenario should be addressed by more detailed calculations.

References

[1] American Society for Testing and Materials, West Conshohocken, Pennsylvania. *ASTM E 1355-04, Standard Guide for Evaluating the Predictive Capabilities of Deterministic Fire Models*, 2004.

[2] W. W. Jones and R. D. Peacock. Technical Reference Guide for FAST Version 18. Technical Note 1262, National Institute of Standards and Technology, 1989.

[3] L. Y. Cooper and G. P. Forney. The Consolidated Compartment Fire Model (CCFM) Computer Application CCFM-VENTS – Part I: Physical Reference Guide. NISTIR 4342, National Institute of Standards and Technology, 1990.

[4] R. W. Bukowski, R. D. Peacock, W. W. Jones, and C. L. Forney. Technical Reference Guide for the HAZARD I Fire Hazard Assessment Method. Version 1.1. Volume 2. NIST Handbook 146/II, National Institute of Standards and Technology, 1991.

[5] R. D. Peacock, W. W. Jones, G. P. Forney, R. W. Portier, P. A. Reneke, R. W. Bukowski, and J. H. Klote. Update Guide for HAZARD I Version 1.2. NISTIR 5410, National Institute of Standards and Technology, 1994.

[6] R. D. Peacock, G. P. Forney, and P. A. Reneke. CFAST – Consolidated Model of Fire Growth and Smoke Transport (Version 6): Technical Reference Guide. Special Publication 1026, National Institute of Standards and Technology, Gaithersburg, Maryland, July 2011.

[7] R. D. Peacock, W. W. Jones, P. A. Reneke, and G. P. Forney. CFAST – Consolidated Model of Fire Growth and Smoke Transport (Version 6): User's Guide. Special Publication 1041, National Institute of Standards and Technology, Gaithersburg, Maryland, December 2005.

[8] R. D. Peacock, K.B. McGrattan, B. Klein, W. W. Jones, and P. A. Reneke. CFAST – Consolidated Model of Fire Growth and Smoke Transport (Version 6): Software Development and Model Evaluation Guide. Special Publication 1086, National Institute of Standards and Technology, Gaithersburg, Maryland, November 2008.

[9] Verification and Validation of Selected Fire Models for Nuclear Power Plant Applications, Volume 5: Consolidated Fire and Smoke Transport Model (CFAST),. NUREG 1824, U. S. Nuclear Regulatory Commission, Office of Nuclear Regulatory Research, Rockville, MD, 2007.

[10] F. P. Incorpera and D. P. DeWitt. *Fundamentals of Heat Transfer*. John Wiley and Sons, 1981.

[11] W. W. Jones, G. P. Forney, R. D. Peacock, and P. A. Reneke. A Technical Reference Guide for CFAST: An Engineering Tool for Estimating Fire and Smoke Transport. Technical Note 1431, National Institute of Standards and Technology, 2003.

[12] R. D. Peacock, G. P. Forney, P. A. Reneke, R. W. Portier, and W. W. Jones. CFAST, The Consolidated Model of Fire Growth and Smoke Transport. Technical Note 1299, National Institute of Standards and Technology, 1993.

[13] W. W. Jones. Modeling Smoke Movement Through Compartmented Structures. *Journal of Fire Sciences*, 11(2):172, 1993.

[14] W. W. Jones. Multicompartment Model for the Spread of Fire, Smoke and Toxic Gases. *Fire Safety Journal*, 9(1):172, 1985.

[15] W. W. Jones. "Prediction of Corridor Smoke Filling by Zone Models. *Combustion Science and Technology*, 35:229, 1984.

[16] W. W. Jones and G. P. Forney. Modeling Smoke Movement Through Compartmented Structures. In *Proceedings of the Fall Technical Meeting of the Combustion Institute, Eastern States Section*, Ithaca, NY, 1991.

[17] R. D. Peacock, G. P. Forney, and P. A. Reneke. Improved Numerics and Structure in CFAST. Unpublished Memorandum, February 1992.

[18] R. D. Peacock. Fix for Chemistry Algorithm in CFAST. Unpublished Memorandum, April 11 1994.

[19] R. D. Peacock. New Convection Algorithm in CFAST. Unpublished Memorandum, January 5 1993.

[20] R. D. Peacock. HCl Deposition. Unpublished Memorandum, January 5 1993.

[21] R. D. Peacock. New Output and History File Formats for CFAST. Unpublished Memorandum, September 9 1993.

[22] W. W. Jones. Internal memo dated February 1996 Announcing Version 3.0 of CFAST. February 1996.

[23] W. W. Jones. Internal memo dated November 1997 Announcing Version 3.1.1 of CFAST. November 1997.

[24] W. W. Jones. Differences in the 4.0.1 Code from the Beta Release of September 1, 1999 to March 1, 2000. March 2000.

[25] Fire Hazard User's Group. Description of the CFAST 1.4 Release. Letter to CFAST Users, December 1991.

[26] Fire Hazard User's Group. Description of the CFAST 1.6 Release. Letter to CFAST Users, October 1992.

[27] Fire Hazard User's Group. Description of the CFAST 2.0 Release. Letter to CFAST Users, October 1993.

[28] Fire Hazard User's Group. Description of the CFAST 2.0.1 Release. Letter to CFAST Users, January 1996.

[29] Fire Hazard User's Group. Description of the CFAST 3.0 Release. Letter to CFAST Users, August 1996.

[30] W. D. Walton. Zone Computer Fire Models for Enclosures. In P. J. DiNenno, D. Drysdale, C. L. Beyler, and W. D. Walton, editors, *SFPE Handbook of Fire Protection Engineering*, chapter 3-7. National Fire Protection Association and The Society of Fire Protection Engineers, Quincy, MA, 3rd edition, 2003.

[31] *NFPA 805, Performance-Based Standard for Fire Protection for Light Water Reactor Electric Generating Plants*. 2004/2005 National Fire Codes. National Fire Protection Association, Quincy, MA, 2001 edition, 2004.

[32] *NFPA 551, Guide for the Evaluation of Fire Risk Assessment*. 2004/2005 National Fire Codes. National Fire Protection Association, Quincy, MA, 2004 edition, 2004.

[33] J. R. Barnett and C. L. Beyler. "Development of an Instructional Program for Practicing Engineers HAZARD I Users. NBS-GCR 90-580, National Institute of Standards and Technology, 1990.

[34] G. P. Forney and W. F. Moss. Analyzing and Exploiting Numerical Characteristics of Zone Fire Models. *Fire Science and Technology*, 14(1 and 2):49–60, 1994.

[35] R. G. Rehm and G. P. Forney. A Note on the Pressure Equations Used in Zone Fire Modeling. NISTIR 4906, National Institute of Standards and Technology, 1992.

[36] W. W. Jones and R. D. Peacock. Using CFAST to Estimate the Efficiency of Filtering Particulates in a Building. NISTIR 7498, National Institute of Standards and Technology, 2008.

[37] D. Drysdale. *An Introduction to Fire Dynamics*. John Wiley and Sons, New York, 1985.

[38] C. Huggett. Estimation of the Rate of Heat Release by Means of Oxygen Consumption Calorimetry. *Journal of Fire and Flammability*, 12:61, 1980.

[39] B. J. McCaffrey. Momentum Implications for Buoyant Diffusion Flames. *Combustion and Flame*, 52:149, 1983.

[40] G. Heskestad. Engineering Relations for Fire Plumes. *Fire Safety Journal*, 7:25–32, 1984.

[41] E. E. Zukoski, T. Kubota, and B. M. Cetegen. Entrainment in Fire Plumes. *Fire Safety Journal*, 3:107 – 121, 1981.

[42] H.R. Baum and B. J. McCaffrey. Fire Induced Flow Field: Theory and Experiment. In T. Wakamatsu, Y. Hasemi, A. Sekizawa, and P. G. Seeger, editors, *Fire Safety Science. Proceedings. 2nd International Symposium*, pages 129–148, Tokyo, Japan, June 13-17 1989. International Association for Fire Safety Science, Hemisphere Publishing Corporation.

[43] D. D. Evans. Calculating Fire Plume Characteristics in a Two Layer Environment. *Fire Technology*, 20(3):39 – 63, 1984.

[44] G. Heskestad. Fire Plumes, Flame Height, and Air Entrainment. In *SFPE Handbook of Fire Protection Engineering*, 3rd Ed. National Fire Protection Association and The Society of Fire Protection Engineers, 2002.

[45] J. G. Quintiere, K. D Steckler, and D. Corley. An Assessment of Fire Induced Flows in Compartments. *Fire Science and Technology*, 4(1), 1984.

[46] K. D Steckler, H.R. Baum, and J. G. Quintiere. Fire Induced Flows Through Room Openings – Flow Coefficients. NBSIR 83-2801, National Bureau of Standards, Gaithersburg, Maryland, March 1984.

[47] B. M. Cetegen, E. E. Zukoski, and T. Kubota. Entrainment in the Near and Far Field of Fire Plumes. *Combustion Science and Technology*, 39(1-6):305–331, 1984.

[48] J. G. Quintiere, K. D Steckler, and B. J. McCaffrey. A Model to Predict the Conditions in a Room Subject to Crib Fires. In *First Specialist Meeting (International) of the Combustion Institute*, Talance, France, 1981.

[49] L. Y. Cooper. Calculation of the Flow Through a Horizontal Ceiling/Floor Vent. NISTIR 89-4052, National Institute of Standards and Technology, 1989.

[50] L. Y. Cooper. Algorithm and Associated Computer Subroutine for Calculating Flow Through a Horizontal Ceiling/Floor Vent in a Zone-Type Compartment Fire Model. NISTIR 4402, National Institute of Standards and Technology, 1990.

[51] L. Y. Cooper. Combined Buoyancy- and Pressure-Driven Flow Through a Shallow, Horizontal Circular VENT. *Journal of Heat Transfer*, 117:659–667, August 1995.

[52] J. H. Klote and J. A. Milke. *Principles of Smoke Management*. American Society of Heating, Refrigerating, and Air-Conditioning Engineers, Inc, Atlanta, GA, 2002.

[53] *2001 ASHRAE Handbook - HVAC Systems and Equipment*. American Society of Heating, Refrigerating, and Air-Conditioning Engineers, Inc, Altanta, GA, 2001.

[54] G. P. Forney. Computing Radiative Heat Transfer Occurring in a Zone Fire Model. NISTIR 4709, National Institute of Standards and Technology, 1991.

[55] R. Siegel and J. R. Howell. *Thermal Radiation Heat Transfer*. Hemisphere Publishing Corporation, New York, 2nd edition, 1981.

[56] H. C. Hottel. *Heat Transmission*. McGraw-Hill Book Company, New York, 3rd edition, 1954.

[57] H. C. Hottel and E. Cohen. Radiant Heat Exchange in a Gas Filled Enclosure: Allowance for Non-uniformity of Gas Temperature. *American Institute of Chemical Engineering Journal*, 4(3), 1958.

[58] T. Yamada and L. Y. Cooper. Algorithms for Calculating Radiative Heat Exchange Between the Surfaces of an Enclosure, the Smoke Layers and a Fire. In *Building and Fire Research Colloquiums*. Building and Fire Research Laboratory, National Institute of Standards and Technology, July 1990.

[59] W. W. Jones and G. P. Forney. "Improvement in Predicting Smoke Movement in Compartmented Structures. *Fire Safety Journal*, 21:269, 1993.

[60] C. L. Tien, K. Y. Lee, and A. J. Stretton. Radiation Heat Transfer. In P. J. DiNenno, editor, *SFPE Handbook of Fire Protection Engineering*, chapter 1-4. National Fire Protection Association and The Society of Fire Protection Engineers, 3rd edition, 2002.

[61] C. L. Tien and G. Hubbard. Infrared Mean Absorption Coefficients of Luminous Flames and Smoke. *Journal of Heat Transfer*, 100:235, 1978.

[62] D. K. Edwards. Radiation Properties of Gases. In W. M. Rohsenow, editor, *Handbook of Heat Transfer Fundementals*, pages 74–75. McGraw-Hill Book Company, 2nd edition, 1985.

[63] H. C. Hottel. Radiant Heat Transmission. In W. H. McAdams, editor, *Heat Transmission*. McGraw-Hill Book Company, New York, 1942.

[64] P. Andersson and P. Van Hees. Performance of Cables Subjected to Elevated Temperatures. In *Fire Safety Science – Proceedings of the Eighth International Symposium*, pages 1121–1132. International Association of Fire Safety Science, 2005.

[65] S.P. Nowlen, F.J. Wyant, and K.B. McGrattan. Cable Response to Live Fire (CAROLFIRE). NUREG/CR 6931, United States Nuclear Regulatory Commission, Washington, DC, April 2008.

[66] A. Atreya. Convection Hear Transfer. In P. J. DiNenno, D. Drysdale, C. L. Beyler, and W. D. Walton, editors, *SFPE Handbook of Fire Protection Engineering*, chapter 1-3. National Fire Protection Association and The Society of Fire Protection Engineers, Quincy, MA, 3rd edition, 2003.

[67] G. H. Golub and J. M. Ortega. *Scientific Computer and Differential Equations, An Introduction to Numerical Methods*. Academic Press, New York, 1989.

[68] W. F. Moss and G. P. Forney. "Implicitly coupling heat conduction into a zone fire model. NISTIR 4886, National Institute of Standards and Technology, 1992.

[69] L. Y. Cooper. Fire-Plume-Generated Ceiling Jet Characteristics and Convective Heat Transfer to Ceiling and Wall Surfaces in a Two-Layer Zone-Type Fire Environment. NISTIR 4705, National Institute of Standards and Technology, 1991.

[70] L. Y. Cooper. Heat Transfer in Compartment Fires Near Regions of Ceiling-Jet Impingement on a Wall. *Journal of Heat Transfer*, 111:455, 1990.

[71] L. Y. Cooper. Ceiling Jet-Driven Wall Flows in Compartment Fires. *Combustion Science and Technology*, 62:285, 1988.

[72] Y. Jaluria and L. Y. Cooper. "Negatively Buoyant Wall Flows Generated in Enclosure Fires. *Progress in Energy and Combustion Science*, 15:159, 1989.

[73] G. Heskestad and H. F. Smith. Investigation of a New Sprinkler Sensitivity Approval Test: the Plunge Test. Technical Report 22485 2937, Factory Mutual Research Corporation, Norwood, MA, 1976.

[74] D. Madrzykowski and R. Vettori. A Sprinkler Fire Suppression Algorithm for the GSA Engineering Fire Assessment System. NISTIR 4833, National Institute of Standards and Technology, 1992.

[75] D. D. Evans. Sprinkler Fire Suppression for HAZARD. NISTIR 5254, National Institute of Standards and Technology, 1993.

[76] D. Madrzykowski. Evaluation of Sprinkler Activation Prediction Methods. In *International Conference on Fire Science and Engineering*, Kowlon, 1995. ASIAFLAM, Interscience Limited.

[77] J. Seader and I. Einhorn. "Some Physical, Chemical, Toxicological and Physiological Aspects of Fire Smokes. In *Sixteenth Symposium (International) on Combustion*, pages 1423 – 1445, Pittsburgh, PA, 1976. The Combustion Institute.

[78] G. W. Mulholland and C. Croarkin. Specific Extinction Coefficient of Flame Generated Smoke. *Fire and Materials*, 24:227, 2000.

[79] F. M. Galloway and M. M. Hirschler. A Model for the Spontaneous Removal of Airborne Hydrogen Chloride by Common Surfaces. *Fire Safety Journal*, 14:251, 1989.

[80] F. M. Galloway and M. M. Hirschler. "Transport and Decay of Hydrogen Chloride: Use of a Model to Predict Hydrogen Chloride Concentrations in Fires Involving a Room-Corridor-Room Arrangement. *Fire Safety Journal*, 16:33, 1990.

[81] K. E. Brenan, S. L. Campbell, and L. R. Petzold. *Numerical Solution of Initial-Value Problems in Differential-Algebraic Equations*. Elsevier Science Publishing, New York, 1989.

[82] R. L. Iman and J. C. Helton. An Investigation of Uncertainty and Sensitivity Analysis Techniques for Computer Models. *Rick Analysis*, 8(1):71–90, 1988.

[83] R. D. Peacock, P. A. Reneke, C. L. Forney, and M. M. Kostreva. Issues in Evaluation of Complex Fire Models. *Fire Safety Journal*, 30:103–136, 1988.

[84] A. Beard. Evaluation of Fire Models: Part I – Introduction. *Fire Safety Journal*, 19:295–306, 1992.

[85] K. A. Notarianni. *The Role of Uncertainty in Improving Fire Protection Regulation*. PhD thesis, Carnegie Mellon University, Pittsburgh, PA, 2000.

[86] N. Khoudja. *Procedures for Quantitative Sensitivity and Performance Validation of a Deterministic Fire Safety Model*. PhD thesis, Texas A & M University, 1988.

[87] G. E. P. Box, W. G. Hunter, and J. S. Hunter. *Statistics for Experimenters, An Introduction to Design, Data Analysis and Model Building*. John Wiley and Sons, New York, 1978.

[88] C. Daniel. *Applications of Statistics to Industrial Experimentation*. John Wiley and Sons, New York, 1976.

[89] A. M. Walker. Uncertainty Analysis of Zone Fire Models. Research Report 97/8, University of Canterbury, New Zealand, 1997.

[90] H. W. Emmons. Why Fire Model? *Fire Safety Journal*, 13:77, 1988.

[91] D. Q. Duong. The Accuracy of Computer Fire Models: Some Comparisons with Experimental Data from Australia. *Fire Safety Journal*, 16:415, 1990.

[92] Verification and Validation of Selected Fire Models for Nuclear Power Plant Applications, Volume 1: Main Report. NUREG 1824, U. S. Nuclear Regulatory Commission, Office of Nuclear Regulatory Research, Rockville, MD, 2007.

[93] *NFPA 72, National Fire Alarm Code*. 2004/2005 National Fire Codes. National Fire Protection Association, Quincy, MA, 2003 edition, 2003.

[94] V. Babrauskas and J. F. Krasny. Fire Behavior of Upholstered Furniture. Monograph 173, National Bureau of Standards, 1985.

[95] V. Babrauskas and R. D. Peacock. Heat Release Rate: The Single Most Important Variable in Fire Hazard. *Fire Safety Journal*, 18:255, 1992.

[96] P. A. Thompson, J. Wu, and E. W. Marchant. Modelling Evacuation in Multi-storey Buildings with Simulex. *Fire Engineering*, 56(185):7–11, 1996.

[97] S. Gwynne, E. R. Galea, P. Lawrence, and L. Filippidis. Modelling Occupant Interaction with Fire Conditions Using the buildingEXODUS Evacuation Model. Technical Report 00/IM/54, University of Greenwich, 2000.